6 Determination of Particle Size

6.1 Microscopic Observation

The most important characteristics of many colloidal dispersions (especially aerosols and dispersions of solid particles in liquids) are the size of the particles. Obvious tools for the sizing (except for emulsions and gas bubbles) are optical and electron microscopes.

6.1.1 Optical Microscopes

There are, in addition to an ordinary microscope, many modifications of optical microscopes, such as a fluorescence microscope (using a sample with fluorescent material), a polarized light microscope, a Brewster angle microscope (Henon and Meunier, 1991; Hönig and Möbius, 1991), a near field optical microscope (Pohl and Courjon, 1993), etc. However, they are not necessarily suitable for particle sizing, but may serve to determine the crystal or homogeneity structure. In particular, they are more powerful in observing the structure of a thin membrane.

There is a limitation, 2 μm or larger, on the optical particle sizing because of the well-known diffraction of the light wave used. But, the recent development of the near field optical microscope has proven to improve the spatial resolution to 20 nm (Jiang et al., 1991).

The idea of the near field technique to overcome the diffraction limitation owes Synge (1928). For the purpose of illustration, consider a double-pinhole screen. Using an ordinary optical system we obtain the diffraction. In order to avoid this diffraction we use an optical fiber as follows. Only one of the pinholes is irradiated by placing the narrow opening of the optical fiber very close to the pinhole or the optical fiber is located near one of the pinholes and locally picks up the transmitted light. We can practically apply this idea. If a very sharp end of a fiber located very close to the sample is used in either the image side or the incident light side and the fiber is scanned over the sample area, the image of the sample can be observed without the diffraction limitation. This limitation does not depend on the wavelength of the light used, as long as the aperture of the fiber is very small and is placed very close to the sample, although the amount of light avail-

able for the observation is accordingly reduced. This is a scanning near field optical microscope and can be used for small particles. A modification of this has been used to observe a sample even in water (Muramatsu et al., 1995). However, the sample to be observed must stay at rest during scanning.

In addition to giving the particle size, the optical microscope provides information about shape, crystal structure, whether the particles are primary or aggregated, and whether different compounds are in the sample.

6.1.2 Transmission Electron Microscope

If the particle is a nanoparticle (size: $1 \sim 100$ nm), the transmission electron microscope can be effectively used with a spatial resolution of a few nm, because the electron beam has a small de Broglie wavelength (Exercise 6.2). If the particle is a crystalline, it can easily give a diffraction pattern. Thus, it is an important tool in the study of disperse systems. For a detailed description of the apparatus and techniques, see Silverman et al. (1971).

The main problem encountered in electron microscopy is to require the sample in an evacuated (10^{-4} mmHg) chamber of the microscope and to be bombarded with electrons of high energy without undergoing changes in structure by minimizing electrostatic charging, melting, evaporation, and decomposition. The process of replication is sometimes used. There may also be a problem if the sample is an insulator and accumulate electric charges.

6.1.3 Scanning Microscope

Even with the use of replication or shadowing techniques, the transmission electron microscope cannot give a stereoscopic view. In a scanning electron microscope (SEM), however, an electron beam is focussed to 5–10 nm across the surface of the sample to emit the low energy secondary electrons, which are drawn towards a collector grid (detector). The output of the detector is used to modulate a cathode ray tube (CRT). The scanning of the CRT is synchronized with the scanning of the sample by the primary electron beam. The big advantage of the low energy of the secondary electrons in SEM is as follows. If the sample is held at an angle to the primary electrons, some scanning parts of the hilly surface may be out of the line-of-sight from the collector grid because of the hills. But the secondary electrons emerging from those parts can be collected at the grid crossing over the hills, although the collected current may be weak. Thus, the three-dimensional image can be formed. The depth of field is very large (300–500 times) compared with that of an optical microscope at the same magnification. The limit of resolution is currently about 5 nm. Many nanoparticles are insulators or semiconductors and need some treatment for the successful observation under SEM to avoid charging-up. Namely, they may have to be coated by a metallic film by evaporating gold, palladium, or their alloy.

In SEM, in addition to the secondary electrons and continuous x-rays, characteristic x-rays and Auger electrons are emitted. These may be used for identification of chemical compositions of the sample. The characteristic x-rays are detected by a solid-state detector. However, SEM is not so sensitive to the elements of low atomic number ($Z < 6$). This incapability may be supplemented by using the Auger electrons (Auger electron spectroscopy). An Auger electron is emitted as follows. When the primary electron in SEM knocks off an electron from an inner shell of an atom in the sample, there appears an unoccupied atomic level in the atomic core. One of the electrons in the higher levels then makes a transition to the empty level by giving up the corresponding energy difference to an electron in one of the outer shells. If this happens, the outer electron is emitted as an Auger electron. Thus, the energy of the Auger electron is characteristic of the atom. If this energy is much lower than those of the secondary electrons, it can be used for the analysis.

The samples in SEM must be in vacuum. But the recently developed scanning tunneling microscope (STM) does not require vacuum. It works in air or even in water. Thus, it can be used to observe chemical reactions near the surface of the sample.

STM was developed by Binning et al. (1982). Electrons may be emitted from a sharp tip of a tungsten needle toward a sample by a small potential difference (~ 10 mV) and they tunnel through the gap between them. The current strongly depends on the width of the gap, and can be used to measure the width or the geometric structure of the surface. When scanning the needle over the sample, the current may be used to control the width by moving the needle by a feed-back mechanism or the change of the magnitude of the current may be measured. The resolution depends on the sharpness of the tungsten tip, but can easily attain that of 1 nm. This device, however, still require the sample to be electrically conducting.

The microcontrol mechanism in STM uses piezo elements. This technique has been used widely in various scanning probe microscopes, such as an atomic force microscope (Binning et al., 1986), a magnetic force microscope (Martin and Wickramasinghe, 1987; Saenz et al., 1987), an electrostatic force microscope (Martin et al., 1988), a friction microscope (Mate et al., 1987), etc. The previously described scanning near field optical microscope also uses the mechanism. As will be easily understood without further description, many of them do not need conducting samples and can be very useful in the study of disperse systems.

6.2 Light Scattering for Particle Sizing

6.2.1 Classical Light Scattering

The classically famous Tyndall effect is due to light scattering by colloidal particles. This light scattering is to be observed at right angles to the incident light and could be used to make very small colloidal particles visible as pin points against dark background in a ultramicroscope. The scattered intensity could give some idea about the particle size.

The exact treatment of the light scattering is not simple, but its limiting cases can be classified in terms of the particle radius a and the wavelength λ of the light in the medium as

$$a < \lambda/20, \text{ Rayleigh scattering,}$$

$$a > 2\lambda, \text{ diffraction theory .}$$

In either case, the observation point is far from the particle.

If the first condition $(a < \lambda/20)$ holds, the electric field of the incident light is almost uniformly in phase everywhere across the particle. For simplicity, we assume that the particle is transparent. All of the atoms in the particle are then equally exposed to the incident light and atomic dipole moments are independently induced. These dipoles are oscillating with the frequency of the incident light and they independently emit radiation (scattered wave) in all directions. In small particles, the scattered waves from the dipoles are nearly in phase at any observation point irrespective of the direction and distance. Therefore, in the Rayleigh regime, the particle can be considered to respond to the incident wave as a one unit and the induced dipole moment can be approximated by Eq. 4.96 or the like (Exercise 6.5). Thus, the interaction with the incident wave can be represented by the particle polarizability. This regime includes only small particles, such as macromolecules.

However, if the particle is larger, this approximation fails to hold and the phase relation among the waves scattered from different atoms of the particle becomes very complex. The overall effect gives rise to maxima and minima in the scattered intensity depending on the scattered direction, with largest intensity in the forward direction of the incident wave. This behavior depends on the particle size. If the size is about the same or smaller than λ, the Rayleigh-Gans-Debye theory may be a good approximation (Kerker, 1969). The scattering of spherical particles can, however, be more rigorously treated with the help of the rigorous Mie theory (Mie, 1908; Garcia-Rubio, 1987). With the advent of high speed computer, the treatment has advanced rapidly. Later Kerker (1969) extended the Mie theory to include cylinders and stratified spheres. These theories must be used whenever the particle size is large.

If the particle size is larger than 2λ, the light scattered with large angles becomes very weak because of destructive interference and only the forward scattering is pronounced (Mie scattering has already this tendency.) This type of scattering is customarily called diffraction. For this diffraction regime, a method has been described by Weiner (1984) to cover observations of spherical particles larger than 1 μm. Since the diffraction pattern spreads more for smaller particles but is narrower in the forward direction for larger particles, the intensity distribution in the diffraction pattern can be used to measure particle sizes in either monodisperse or polydisperse systems.

6.2.1.1 Rayleigh and Rayleigh-Gans-Debye Scattering

In 1871 Rayleigh obtained an approximate equation for the scattered intensity, I_θ. Consider that an unpolarized light of intensity $I_{i,u}$ and wavelength λ is incident on a single small isotropic particle at rest in vacuum. Using the particle polarizability, α (assumed to be real), which is defined by following the atomic polarizability described in Sec. 4.2, he found that

$$\frac{I_\theta}{I_{i,u}} = \frac{8\pi^4}{\lambda^4 R^2}\left(\frac{\alpha}{4\pi\varepsilon_0}\right)^2 (1+\cos^2\theta) \tag{6.1}$$

where the angle θ is measured in the plane of the incident and scattered beam (the plane of acattering) and I_θ is the intensity at a distance R from the particle (see Fig. 6.1). In Eq. 6.1, the terms, 1 and $\cos^2\theta$ refer, respectively, to the incident light with the polarization vector perpendicular (vertical) and parallel (horizontal) to the plane of scattering. Note that α is proportional to the volume of the particle.

If N identical isotropic particles are exposed to the incident light in a medium of refractive index n_m (see Exercise 6.5), Eq. 6.1 can easily be rewritten for the scattered intensity I_θ by multiplying Eq. 6.1 by N, but the wavelength is now λ_0/n_m, where λ_0 is the wavelength in vacuum, provided the concentration is low.

In Eq. 6.1, I_θ is proportional to the square of the volume of the particle. Therefore, the scattered intensity must increase if the particles are subject to aggregation (called coagulation or flocculation), nucleation, etc.

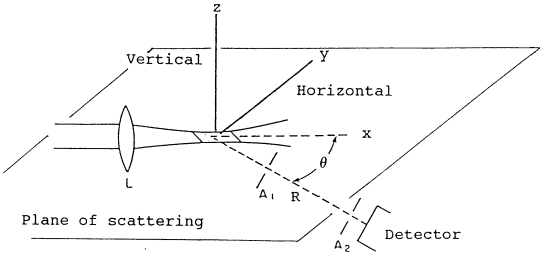

Fig. 6.1 The scattering geometry. A_1,A_2: Apertures, R,x,y: in the plane of scattering.

Equation 6.1 holds for small isotropic particles. It can be used when the dispersed solution is flowing. If the scattered intensity is monitored by a photomultiplier, it easily exhibits the particle size distribution as the solution passes by the device and can be used for a quality control of the size distribution for small particles ($a < 1$ μm) (Cummins 1983).

Because of the scattering, even though there is no absorption (α is real) in its true sense, the incident wave loses its intensity as it is transmitted through a medium containing suspended particles. The time-averaged attenuation obeys the exponential law, if it is dilute,

$$I(x) = I_0 \exp[-(\tau_p + \tau_m)x] \tag{6.2}$$

where the x axis is in the direction of the incident light and I_0 is the intensity at $x=0$. The exponent, $\tau_p + \tau_m$, is called the turbidity or attenuation of the solution.

The value of τ_p can be experimentally obtained by subtraction of τ_m from the turbidity when particles are present in the solution. If the size of suspended particles is small, an exact theoretical expression for τ_p can be derived by using Rayleigh scattering formula. We may make an approximation by assuming the solution is a continuous medium, so that we introduce the index of refraction for the solution, n_s. Then, as long as the index of refraction is uniform in the solution, there should be no light scattering. However, Brownian motion of the discrete particles causes local fluctuations in the particle concentration c (mass per unit volume), and, accordingly, in the index of refraction of the solution. In reality, there are many small regions where the particle concentrations are different from surroundings, and the fluctuations occur since particles are moving in and out one by one to and from the small regions. This discrete behavior introduces the local change of the effective polarizability by the amount corresponding to one particle (or, similarly, to one molecule in the medium). Thus, from Exercise 6.6, for the part of the particle fluctuation,

$$\alpha = 2\varepsilon_0(n_s - n_m)/(n_m N_p) = 2\varepsilon_0(\partial n_s/\partial c)(m/n_m) \tag{6.3}$$

where $c = N_p m$, N_p and m being the number density and mass of the particle. (If we use the molecular weight, M, of the particle, $c = N_p M/N_A$, N_A being the Avogadro number.) Equation 6.3 may be introduced in Eq. 6.1, which is averaged over the angles to obtain the turbidity τ_p by remembering that τ_p is due to the unit scattering volume. Hiemenz (1986), however, treated the fluctuations of n_s more rigorously by using a statistical mechanics to obtain

$$\tau_p \frac{32\pi^3 n_m^2}{3N_A \lambda_0^4} \left(\frac{dn_s}{dc}\right)^2 \frac{1}{(1/cM) + 2B} \tag{6.4}$$

where B denotes the second virial coefficient of the osmotic pressure of the solution. B characterizes the interactions among particles in the density fluctuation. (The osmotic pressure, $\Pi = RTc^2\{(1/Mc) + B\}$, works locally to bring the fluctu-

ating concentration to equilibrium.) The quantity, λ_0, is the wavelength in vacuum ($\lambda_0 = n_m\lambda$). Equation 6.4 gives a particle mass irrespective of the shape for small particles. For a polydisperse systems, Eq. 6.4 provides a weight-averaged molecular weight, $M_{av} = (\sum c_i M_i)/\sum c_i = (\sum N_i M_i^2)/(\sum N_i M_i)$. For the distribution of the size, see Chapt. 7.

When the particle is larger or nonspherical, Eq. 6.1 is modified by introducing a correction factor like in the Rayleigh-Gans-Debye theory. If nonspherical, the particle polarizability is a tensor (Eq. 6.17) and the scattered wave is polarized in a different direction from the incident polarization. If the incident light is linearly polarized, the scattered light is then partially depolarized. For the time being, however, we simply ignore this partial depolarization. If the particle size is large, the scattering is strongly angular dependent. In order to experimentally treat this case, we consider that the scattering occurs from the scattering volume V_s, which contains N particles (the number density: N/V_s). The differential cross-section, or Rayleigh ratio, per unit volume in the scattering, is defined by, in a dilute solution,

$$\mathcal{R}_\theta = R^2 I_\theta/(V_s I_{i,v}) \tag{6.5}$$

where I_θ is the scattered intensity in the scattering angle θ from the scattering volume V_s when an incident light wave has the "vertical" polarization. (The polarizability of Eq. 6.1 may be replaced by Eq. 6.3 and I_θ =[I_θ per particle]·N/V_s) We, again, imply that Eq. 6.5 is the result after subtraction of the scattered light due to the medium alone. Note that $\mathcal{R}_\theta$ can be determined by experiments. If interparticle interactions are present, the coefficient B must be included and Eq. 6.5 must be related as follows: for a "vertically" polarized light,

$$\frac{Hc}{\mathcal{R}_\theta} \simeq \left[\frac{1}{M} + 2Bc\right]\frac{1}{P(\theta)} \tag{6.6}$$

$$H = \frac{4\pi^2 n_s^2}{\lambda_0^4 N_A}\left(\frac{\partial n_s}{\partial c}\right)^2 \tag{6.7}$$

Here, $P(\theta)$ is the Debye factor (Debye, 1947). If the incident light is "unpolarized", the coefficient becomes 2 instead of 4 in H.

The factor, $P(\theta)$, takes care of the intraparticle interference (within a particle). Suppose that the incident wave propagates in the solution in the direction of a unit vector $\boldsymbol{n}_0$, behaving at position $\boldsymbol{x}_j$ and time t, like $\exp(ik\boldsymbol{n}_0\cdot\boldsymbol{x}_j - i\omega t)$, where $k = 2\pi/\lambda$, λ being the wavelength in the solution. The wave induces dipole moment on atoms in the particle. (We assume that both the atoms and the particle are at rest.) An induced dipole at $\boldsymbol{x}_j$ emits a wave, as a scattered wave, with the same phase as the incident wave at $\boldsymbol{x}_j$. The scattered wave leaves the atom with the same phase as the incident wave, $\exp(ik\boldsymbol{n}_0\cdot\boldsymbol{x}_j - i\omega t)$. Then, what will be the phase when it reaches at the observer at $\boldsymbol{x}$? We will find in the following this

phase and compare the phase with that of the scattered wave from another atom at $\boldsymbol{x}_i$ of the particle. We choose the origin of the coordinates at the center of the particle.

In the following discussion we note that the same time factor, $\exp(-i\omega t)$, appears everywhere, so that the time factor will be omitted for the time being, but must be recalled if necessary.

The scattered wave from the atom at $\boldsymbol{x}_j$ is a spherical wave, $\exp(ik|\boldsymbol{x}-\boldsymbol{x}_j|)/|\boldsymbol{x}-\boldsymbol{x}_j|$, around $\boldsymbol{x}_j$ as observed at $\boldsymbol{x}$. Its phase at $\boldsymbol{x}_j$ is already $\exp(ik\boldsymbol{n}_0\cdot\boldsymbol{x}_j)$. Since $|\boldsymbol{x}a| \gg |\boldsymbol{x}_j|$ (the atom is inside the small particle), $|\boldsymbol{x}-\boldsymbol{x}_j| \approx |\boldsymbol{x}| = R$ (the distance between the particle and the observer). This approximation, however, cannot be used in the oscillating exponential function. Since $|\boldsymbol{x}-\boldsymbol{x}_j| = ((\boldsymbol{x}-\boldsymbol{x}_j)\cdot(\boldsymbol{x}-\boldsymbol{x}_j))^{1/2} \approx R(1-\boldsymbol{x}\cdot\boldsymbol{x}_j/R^2) = R(1-\boldsymbol{n}_s\cdot\boldsymbol{x}_j/R)$, $\boldsymbol{n}_s$ being the unit vector in the direction of the observation, the scattered wave, which is observed at $\boldsymbol{x}$, has the following form (remember the initial phase of $\exp(ik\boldsymbol{n}_0\cdot\boldsymbol{x}_j)$):

$$\text{Scattered } \boldsymbol{E}_s = \boldsymbol{A}_0 \frac{e^{ikR}}{R} e^{ik(\boldsymbol{n}_s-\boldsymbol{n}_0)\cdot\boldsymbol{x}_j} f(\theta) \tag{6.8}$$

where $f(\theta) = 1$ (vertical) or $\cos\theta$ (horizontal polarization) and $\boldsymbol{A}_0$ is the amplitude depending on the atomic polarizability and the intensity of the incident light. In Eq. 6.8, the factor, $\exp(ikR)f(\theta)/R$, leads to the Rayleigh scattered wave, since the additional factor is of order of unity for small particles as will be seen later. This factor has the phase which depends on the position, $\boldsymbol{x}_j$, of the j-th atom of the particle.

There are many atoms in the particle and all of them equally scatter the light with respective phases. The scattered waves from those atoms are observed to interfere each other. The interference appears in the sum of Eq. 6.8 over the atoms and the intensity is given by the absolute square. Thus, the angular dependence of the intensity at the observer is expressed in the structure factor:

$$F(q) = (1/N^2)\left|\sum_j \exp(i\boldsymbol{q}\cdot\boldsymbol{x}_j\right|^2 \tag{6.9}$$

where N is the number of atoms in the particle and $\boldsymbol{q} = k\boldsymbol{n}_s - k\boldsymbol{n}_0$ is the vectorial change in the wave vector at the scattering, called as the scattering vector. The angle between $\boldsymbol{n}_0$ and $\boldsymbol{n}_s$ is the scattering angle, θ. The magnitude of $\boldsymbol{q}$ is given by

$$|\boldsymbol{q}| = q = 2k\cdot\sin(\theta/2) \tag{6.10}$$

The structure factor stands for the intraparticle interference. It is the Debye factor $P(\theta)$ and may be calculated by replacing the summation by an integral in Eq. 6.9. We note that, even when the particles are nonspherical, only the angle-averaged value over the orientation of the particles is observed. Therefore, we can simplify the integral. The results of $P(\theta)$ are given for various shapes in Table 6.1. Note that λ is the wavelength in the solution.

Table 6.1 Scattering structure factors, $P(\theta)$, for various shapes, averaged over the orientation distribution.

Sphere of radius, a (Rayleigh, 1914; Pusey, 1982).

$$F(q) = \Phi(x) = [3\{\sin(x) - x \cdot \sin(x)\}/(x)^3]^2 , \quad x = qa$$

Ellipsoid of revolution of semiaxes, a, a, va, (Guinier, 1939).

$$F(\theta) = \int_0^{\pi/2} \Phi(x) \cos\theta \mathrm{d}\theta , \quad x = qa\sqrt{\cos^2\theta + v^2 \sin^2\theta}$$

Cylinders of revolution of radius, a, and height, $2h$, (Fournet, 1951).

$$F(q) = \int_0^{\pi/2} \frac{\sin^2(qh\cos\theta)}{(qh\cos\theta)^2} \frac{4J_1^2(qa\sin\theta)}{(qa\sin\theta)^2} \sin\theta \mathrm{d}\theta , \quad \text{Bessel function of order 1}$$

Flat disc of infinitesimal thickness and radius, a, (Kratky and Porod, 1949).

$$F(q) = \frac{2}{(qa)^2}\left[1 - \frac{J_1(2qa)}{qa}\right]$$

Rod of infinitesimal transverse dimensions and length, $2l$, (Neugebauer, 1943).

$$F(q) = \frac{1}{ql}\int_0^{2ql} \frac{\sin(x)}{x} \mathrm{d}x - \left[\frac{\sin(ql)}{ql}\right]^2$$

Flexible chain of mean square length, $\langle l^2\rangle^{1/2}$

$$F(q) = \frac{2}{x^4}[x^2 - 1 + \mathrm{e}^{-x^2}] , \quad x = q\langle l^2\rangle^{1/2}/6$$

The Debye factor, as given by Eq. 6.9, depends on θ, through $\boldsymbol{q}$, and the distribution of the atoms ($\boldsymbol{x}_j$) in the particle. If the particles are spherically symmetric or if they have random orientations and averaged over the distribution, $P(\theta)$ depends only on q and the distances between the atoms in the same particle. In Eq. 6.9, by expanding $\exp(i\mathbf{q}\cdot x_j)$ in terms of spherical Bessel functions (Exercise 6.8), we have

$$P(\theta) = F(q) = (1/N^2)\sum_i \sum_j \sin(qr_{ij})/(qr_{ij}) , \quad r_{ij} = |\boldsymbol{x}_i - \boldsymbol{x}_j| \qquad (6.11)$$

If the particle size is smaller than $\lambda/20$, $P(\theta) \sim 1$. For small particles such that $qr_{ij} < 1/3$,

$$P(\theta) = 1 - (1/N^2)\sum_i \sum_j (qr_{ij})^2/3 + \ldots = 1 - a_G^2 q^2/3 + \ldots , \quad (a_G q < 1) \qquad (6.12)$$

where a_G is the radius of gyration given in Table 4.1.

In Eq. 6.6, $P(\theta)$, M, and B are unknown and must be determined from the experimental data. For small θ, $P(\theta) \sim 1$ and unknown constants, M and B, may be obtained by changing c. $P(\theta)$ can then be determined for various θ. However, the accurate measurements for small θ are difficult. The extrapolation can be conveniently made by the Zimm plot (Zimm, 1948; Evans, 1972). This is to plot $Hc/\mathcal{R}_\theta$ against $\sin^2(\theta/2) + Kc$ for various values of θ and c, where the value of K is so chosen by trial and ereror to evenly spread out the data points. (A good trial estimate of K is such that $K = 0.8/c_{\max}$, $c_{\max}$ referring to the highest concentration used.) The above mentioned choice of the variables in this plot is due to the reason that by combining Eqs. 6.6, 6.10, and 6.12 we have

$$\frac{Hc}{\mathcal{R}_\theta} \simeq \frac{1}{M} + \frac{(2ka_G)^2}{3M} \sin^2\left(\frac{\theta}{2}\right) + 2Bc$$

In the plot, each point corresponds to a particular value of c, θ values. From this equation we see that the points standing for the same values of c and those for the same values of θ are on straight lines, respectively. (There are different lines for different vales of c or θ.) Hence, the extrapolations, $c \to 0$ and $\theta \to 0$, are easily made to give the value of 1/M.

Through this analysis, differences in shape may be predicted, but the use of $P(\theta)$ to asses shape when unknown or size for known shape is limited. Recently, Watson and Jenings (1991) have calculated $P(\theta)$ for randomly oriented two-dimensional scatterers, such as disk, rectangle, square, triangular, hexagonal shaped particles with negligible thickness, including the interference in the scattered waves from them.

If the Debye factor must be included in the light scattering, Eq. 6.1 must be multiplied by $P(\theta)$. Since $P(\theta)$ depends on both the particle size and q, if the scattered intensity is observed as a function of q or θ the size distribution of particles can be found (Schnablegger and Glatter, 1991), see Chapt. 7.

If the scattering is observed under a strong external electric field, the intensity is different from that without the field and this difference can provide a sensitive method for the shape and size determination of a certain type of particles. In the presence of an externally applied static field, $\boldsymbol{E}$, the Debye factor changes to $P_E(\theta)$. Consider nonspherical particles, which do not have a permanent dipole moment. Then, they align under a strong $\boldsymbol{E}$ with their major particle dimension along $\boldsymbol{E}$. If they have a permanent dipole moment, its effect under $\boldsymbol{E}$ may be isolated by using an oscillating electric field with a frequency of typically a few kilohertz, which is above the critical Debye frequency for particle orientation relaxation. Thus, the dispersed particles can be aligned (just in the one direction) with the external field and the Debye factor $P_E(\theta)$ to be used in the scattering must be different from that for a randomly oriented system. Kaolin and talc particles used in the paper industry, silver halides used in photographic film, and synthetic pigments in paint have a flat or tabular shape, for which Watson and Jennings (1993) introduced a theoretical treatment of the light scattering under a strong electric field.

6.2.1.2 Mie Scattering

When $a \sim$ or $>\lambda$, we must use the complete Mie theory, which is, however, strictly applicable only to spheres. Computer matching of the theoretical scattering pattern with experimental data has been used by Kerker (1969).

If the particle has a general shape and size, we may start from the general theory of scattering (see, for instance, Jackson, 1975).

6.2.2 Frequency Broadening and Photon Correlation

Now we consider that the particles make thermal motion in solution. The motion is described, in Chapt. 4, as the translational and rotational Brownian motion, and is known to modify the frequency of the scattered light by the particles, depending on the particle size, shape, and mutual interactions. The experimental procedures of sizing are described by Pecora (1985) and Chu (1991). We consider in this chapter only monodisperse systems of identical particles and postpone polydisperse cases to Chapt. 7.

6.2.2.1 Brownian Motion and Frequency Broadening

The particles in colloidal solutions make Brownian motion and the scattered wave by them is observed with a frequency broadening. This frequency broadening observed with the solutions are usually not due to the Doppler effect. First of all, the magnitude of the Doppler broadening is usually very different from those of the observed broadening. If the colloidal solution is in motion as a whole, or the particles are uniformly moving due to a concentration gradient, or, when ionized, due to an external steady electric field, the frequency modification occurs due to the motion, but does not lead to the broadening. Secondly, if it is the Doppler broadening the broadened line shape must reflect the velocity distribution (Gaussian) of the thermal motion of the particles in the solution. The typical experiment shows that the frequency broadening has a Lorentzian line shape.

In contrast, Doppler broadening may be important in scattering due to aerosols since collisions with other molecules and other aerosols are rare (Ancellet and Menzies, 1987).

Suppose that the j-th Brownian particle has an instantaneous velocity, $\boldsymbol{v}_j(t)$. The wave scattered by this particle behaves at the detector, if the solution is dilute, as (see Eq. 6.8)

$$\boldsymbol{E}_{\mathrm{s}}(t) = \sum_j \boldsymbol{E}_{\mathrm{s},j}(t) \mathrm{e}^{i[\boldsymbol{q}\cdot\boldsymbol{x}_j(o) + \int_0^t \boldsymbol{q}\cdot\boldsymbol{v}_j(t)\mathrm{d}t] - i o_0 t} \tag{6.13}$$

where $\boldsymbol{E}_{\mathrm{s},j}$ is the amplitude vector of the scattered wave by the j-th particle. The frequency, ω_0, is that of the incident light. The vector, $\boldsymbol{q}$, is the scattering vector, $\boldsymbol{q}=k(\boldsymbol{n}_{\mathrm{s}}-\boldsymbol{n}_0)$ as before.

The integral in the exponent of Eq. 6.13 gives a Doppler frequency shift of $\boldsymbol{q}\cdot\boldsymbol{v}_j$ during the time interval over which the velocity is constant, so that the scattered frequency is $\boldsymbol{q}\cdot\boldsymbol{v}_j-\omega_0$.

The scattering vector, $\boldsymbol{q}$, is common to all scatterer and remains constant in an observation, but $\boldsymbol{E}_{s,j}$ and $\boldsymbol{v}_j$ (and, consequently, $\boldsymbol{q}\cdot\boldsymbol{v}_j$) are, in general, randomly changing in time, in magnitude and direction, due to Brownian motion. The abrupt change in $\boldsymbol{q}\cdot\boldsymbol{v}_j\Delta t$ causes an abrupt phase shift, where Δt is a Brownian collision duration, during which a kink in the Brownian pathway occurs (see Fig. 5.2). The abrupt phase shift is often large compared with unity in radian. Even if it is small, it can add up to unity or even more after many small abrupt phase shifts. When such a large phase shift, single or accumulated, occurs, the incident long wave train is divided into two incoherent shorter wave trains (Ch'en and Takeo, 1957). If this collisional effect occurs successively, the scattered light is divided into many wave trains of random length. The shortening of the wave trains results in frequency broadening in the frequency domain (Exercise 6.10 or a frequency uncertainty $\Delta\omega\sim 2\pi/\Delta t$, Δt being here the length of the wave train in time), and the unpredictable redistribution of incident photons among the divided wave trains results in a fluctuating scattered intensity in the time domain. How the random phase shifts affect the intensity can be classically seen as follows.

For simplicity, instead of treating the time sequence of the behavior, consider the light waves scattered by many particles. Then, the electric field of the waves at the detector is given by

$$E(t)=\sum_j E_{s,j}\exp(-i\omega_0 t+i\phi_j(t))=E_s\exp(-i\omega_0 t)\cdot A(t)\exp(i\phi(t)) \tag{6.14}$$

where we assume that all the waves have the same polarization and the same real amplitude, E_s, irrespective of j ($E_{s,j}=E_s$). The last factor in Eq. 6.14 is obtained by

$$A(t)^2=\left\{\sum_j\cos(\phi_j(t))\right\}^2+\left\{\sum_j\sin(\phi_j(t))\right\}^2$$

and

$$\tan(\phi(t))=\left\{\sum_j\sin(\phi_j(t))\right\}\Big/\left\{\sum_j\cos(\phi_j(t))\right\}$$

The intensity is given by $I(t)=(c/8\pi)|E(t)|^2=(c/8\pi)E_s^2A^2(t)$, where c is the speed of light. Thus, the random phase shifts result in the random amplitude modulation. (Note here that taking a half of the real part of $E^*(t)E(t)$ is equivalent to take the average over one cycle of the oscillation (Jackson, 1975, p. 241).)

We note that, in order to experimentally observe the frequency broadening, the scattering volume used must be many times larger than the volume which can hold the average Brownian displacement, r, during which the particle scatters an uninterrupted wave train. We have found in Sec. 4.1.1 that this r is about the scattering length, q^{-1}. Thus, it is interesting to note that the size of the important r depends on the wavelength and, from Eq. 4.6, $r \sim (Dt)^{1/2} \sim q^{-1}$ or $q^2Dt \sim 1$, where t is the length in time of the Brownian-shortened wave train. It results in the frequency broadening of q^2D. The Brownian collision obeys the Poisson statistics, so that the line shape is Lorentzian, slightly modified by the Gaussian statistics of the Doppler broadening due to moving particles.

The observation of the frequency distribution of the scattered wave may be made by means of various classical optical devices, like a high-resolution spectrograph, an interferometer, etc. But, equivalently, the fluctuating intensity of the scattered light may be observed electronically by a photomultiplier, which is capable to respond to a variation of intensity as fast as ten picosecond. If the fluctuation is too fast for an available electronic device, the optical method is useful.

A photomultiplier is a nonlinear device. The photocathode emits photoelectrons, by mixing waves, according to the incidence of $|\sum_i E_i(\omega)|^2$, as long as the fields are coherent, whatever the course (route) of the incident light may be. Each Brownian particle in a scattering volume is exposed to the same incident light, but scatters independently. How do the scattered waves from the particles behave at the photocathode? Jakeman et al. (1970) theoretically analyzed the behavior. If the surface area of the detector is less than the coherent area, defined by

$$A_{\text{coh}} = \frac{\lambda^2 R^2}{\pi a^2} \tag{6.15}$$

the scattered waves reaching the detector behave as a single wave at the detector. In Eq. 6.15, λ and R are, respectively, the wavelength in the medium and the distance between the detector and the scattering volume of radius a. If the detector size is equal to the coherent area, the observation exhibits a largest intensity fluctuation.

Equation 6.15 can be intuitively obtained. For simplicity, suppose that the cross-sectional area of the scattering volume normal to the direction of the observation is a square of side length l. Consider, in analogy, this area as the area of a pinhole. Then, the light diffracted within the first (central) diffraction region is coherent and the solid angle of the light spread in the zone is called as the coherent solid angle, given by λ^2/l^2. This relation can also be obtained by the uncertainty in the wavenumber because of the finite size of the pinhole. Namely, the uncertainty, Δk, along the direction of one side of the pinhole is $2\pi/l$ (the uncertainty relation in wave: $\Delta k \cdot (l/2\pi) \sim 1$). This uncertainty gives rise to an uncertainty in the propagation of the scattered wave. In a case of one dimensional slit, waves propagating within the angle, $a = \Delta k/k = \lambda/l$, in Fig. 6.2 remains coherent if they leave the slit as coherent. For a square pinhole, the angle becomes as the above solid angle. Thus, for a circular pinhole of radius a, we have

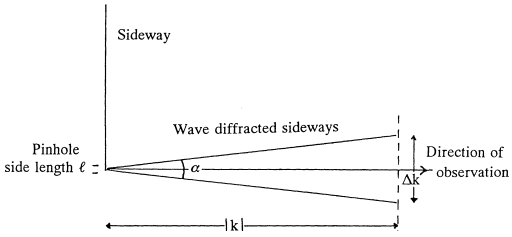

Fig. 6.2 Coherent angle.

$$\Omega_{\text{coh}} = \lambda^2/\pi a^2 \tag{6.16}$$

If the detector just covers this solid angle, i.e., if the detector area is equal to A_{coh} (Eq. 6.15), the intensity fluctuation is most effectively observed. (For more details, see Chu, 1991.)

6.2.2.2 Autocorrelation Function and Line Shape for a Symmetric Top (Dilute Monodisperse Systems)

In an ensemble, if any quantity behaves in time like $x(t)=x_0\exp[-i\omega_0 t+i\phi(t)]$, where $\phi(t)$ varies slowly compared with the carrier frequency, ω_0, then the product, $x^*(t)x(t+\tau)=x_o^2\cdot\exp(-i\omega_0\tau)\ \exp[-i\phi(t)+i\phi(t+\tau)]$, contains only slowly varying component. If $\phi(t)$ has a random-noise component, it cancels out on averaging the product with respect to time. This is an autocorrelation function and can extract slowly varying physical components, such as a relaxation process of an abrupt thermal fluctuation followed by returning to equilibrium. The autocorrelation function sometimes occurs as a natural procedure with a nonlinear detector, such as a diffraction grating, which works as a device of taking the Fourier transform of the autocorrelation function and show a frequency broadening.

If particles are identical and do not interfere each other in the scattering process, we can treat each scattered wave separately in the summation of Eq. 6.13. This occurs in the dynamic scattering, since the particles are considered to individually undergo a random walk. Namely, the scattered intensity is proportional to

$$(1/N^2)\sum_j\sum_{j'}\exp[i\boldsymbol{q}\cdot(\boldsymbol{x}_j(t)-\boldsymbol{x}_{j'}(t))]$$

where N is the number of particles in the scattering volume and the summations are on the particle positions. If j and j' refer to different particles, the summations vanish, unless particle motions are correlated somehow, say, due to interparticle interactions. In the following, we assume a dilute monodisperse system and treat the dynamic effect of individual particles on scattering.

In general, the particle polarizability, $\overleftrightarrow{\boldsymbol{\alpha}}$, is a tensor fixed to the particle and rotates in space due to collisions (see Sec. 4.1.2). If the amplitude of the incident

light is denoted by $\boldsymbol{E}_i$, the induced dipole moment is given by, if the particle is at rest,

$$\boldsymbol{p} = \overleftrightarrow{\boldsymbol{\alpha}} \cdot \boldsymbol{E}_i \tag{6.17}$$

Then, even though $\boldsymbol{E}_i$ is fixed in space, the amplitude, $\boldsymbol{E}_{\mathrm{s},j}$, of the scattered light is polarized along $\boldsymbol{p}$ and changes, as $\overleftrightarrow{\boldsymbol{\alpha}}$ rotates.

We do not consider the case of fluctuating $\overleftrightarrow{\boldsymbol{\alpha}}$ due to instability, chemical reactions, flocculation, etc. (see Berne and Pecora, 1976; Pecora, 1985).

The reduced scattered wave from the j-th particle observed at the detector is written from Eq. 6.13 as

$$\boldsymbol{E}_j(t) = \boldsymbol{E}_{\mathrm{s,j}}(t) \exp(i\boldsymbol{q} \cdot \boldsymbol{x}_j(t) - i\omega_0 t)/E_i^0 \tag{6.18}$$

where E_{i}^0 is the amplitude of the incident wave. The intensity in the frequency domain is given by (Exercise 6.16)

$$I_j(\omega)\mathrm{d}\omega \propto \omega^4 |\hat{\boldsymbol{E}}_j(\omega)|^2 \mathrm{d}\omega = \omega^4 \hat{\boldsymbol{E}}_j^*(\omega) \cdot \hat{\boldsymbol{E}}_j(\omega)\mathrm{d}\omega \tag{6.19}$$

where $\hat{\boldsymbol{E}}_j(\omega)$ is the Fourier transform of $\boldsymbol{E}_j(t)$. In the following, we can ignore the ω^4 dependence since ω is nearly constant in the frequency range of the broadening. Hence,

$$I_j(\omega)\mathrm{d}\omega \propto \frac{1}{2\pi} \int_{-\infty}^{\infty} \mathrm{d}t_1 \int_{-\infty}^{\infty} \mathrm{d}t_2 \, \boldsymbol{E}_{\mathrm{s},j}^*(t_1) \cdot \boldsymbol{E}_{\mathrm{s},j}(t_2) \mathrm{e}^{-i\boldsymbol{q}\cdot(\boldsymbol{x}_j(t_1)-\boldsymbol{x}_j(t_2)) - i(\omega-\omega_0)(t_1-t_2)} \mathrm{d}\omega$$

Note that the quantity, $\Delta\omega = \omega - \omega_0$, is the frequency measured from ω_0. By changing variables by $t_1 - t_2 = \tau$ and $t_2 = t_0$, we have

$$I_j(\Delta\omega)\mathrm{d}\Delta\omega \propto \frac{1}{\pi} \mathcal{R} \int_0^{\infty} \mathrm{d}\tau \psi_j(\tau) \mathrm{e}^{-i\Delta\omega\tau} \mathrm{d}\Delta\omega \tag{6.20}$$

where $\mathcal{R}$ is the real part and

$$\psi_j(\tau) = \int_{-\infty}^{\infty} \mathrm{d}t_0 \boldsymbol{E}_{\mathrm{s},j}^*(t_0 + \tau) \cdot \boldsymbol{E}_{\mathrm{s},j}(t_0) \mathrm{e}^{-i\boldsymbol{q}\cdot(\boldsymbol{x}_j(t_0+\tau)-\boldsymbol{x}_j(t_0))} \tag{6.21}$$

Note that $\boldsymbol{E}_{\mathrm{s},j}$ is the reduced field, referring to the unit incident field. The function, $\psi_j(\tau)$, is called the autocorrelation function.

The integration over t_0 in the autocorrelation function implies an averaging process over t_0. What happens during τ after t_0 is averaged by this integral. Namely,

the value of the integrand is averaged over the distributions of the displacement, $(\boldsymbol{x}_j(t_0+\tau)-\boldsymbol{x}_j(t_0))$, and of the rotational behavior of $\boldsymbol{E}_{s,j}(t_0)$ to $\boldsymbol{E}_{s,j}(t_0+\tau)$ due to Brownian motion during a parameter τ. These two averaging processes, $\langle \exp(-i\boldsymbol{q}\cdot(\boldsymbol{x}_j(t_0+\tau)-\boldsymbol{x}_j(t_0))) \rangle$ and $\langle \boldsymbol{E}^*_{s,j}(t_o+\tau)\cdot\boldsymbol{E}_{s,j}(t_0) \rangle$, are independent. Assuming that all the particles behave in the same way in the statinary Brownian motion, the average can be taken, instead of over t_0, over the particle positions at an arbitrarily chosen time t_0, say, 0. We can also omit the particle identification number, j.

The distribution function of the Brownian displacement, $\boldsymbol{r}=\boldsymbol{x}(\tau)-\boldsymbol{x}(0)$, during τ is given by Eq. 4.28 ($t \to \tau$). Thus, for monodisperse systems,

$$\langle e^{-i\boldsymbol{q}\cdot\boldsymbol{r}} \rangle = \int_{-\infty}^{\infty} e^{-i\boldsymbol{q}\cdot\boldsymbol{r}} F(\boldsymbol{r},\tau) d\boldsymbol{r} = \frac{1}{(2\pi)^3} \int_{-\infty}^{\infty} d\boldsymbol{k} \int_{-\infty}^{\infty} d\boldsymbol{r} e^{i(-\boldsymbol{q}\cdot\boldsymbol{r}+\boldsymbol{k}\cdot\boldsymbol{r})-k^2 D\tau}$$

Since

$$\int_{-\infty}^{\infty} e^{i(-\boldsymbol{q}\cdot\boldsymbol{r}+\boldsymbol{k}\cdot\boldsymbol{r})} d\boldsymbol{r} = (2\pi)^3 \delta(\boldsymbol{q}-\boldsymbol{k})$$

the correlation function for the translational part is given by

$$\langle e^{-i\boldsymbol{q}\cdot\boldsymbol{r}} \rangle = e^{-q^2 D\tau} \tag{6.22}$$

This is normalized such that $\langle \exp(-i\boldsymbol{q}\cdot\boldsymbol{r}) \rangle \to 1$ as $\tau \to 0$.

Averaging over the particle rotation needs the distribution function, i.e. the solution of the rotational diffusion equation, Eq. 4.55. The three principal components of the diffusion tensor may be all different, but we consider the symmetric case, where $D^r_{XX}=D^r_{YY} \equiv D^r_\perp$ and $D^r_{ZZ} \equiv D^r_\parallel$. The solution is then given by Eq. 4.64. The particle polarizability tensor may also have the same symmetry, but the symmetry axes of the diffusion tensor and the polarizability tensor may not coincide. If they coincide like in the case of a true symmetric top, the particle rotation around the body-fixed Z axis does not introduce any change in the induced dipole moment and, therefore, only $D^r_\perp$ is important.

In light scattering, $\boldsymbol{p}$ and $\boldsymbol{E}_i$ are referred to a space-fixed coordinate system (Oxyz), because they are related to the quantities observed in space. But, the polarizability, $\overleftrightarrow{\alpha}$, is body-fixed. In general, if the particle has a center of inversion or a plane of symmetry (optically inactive), $\overleftrightarrow{\alpha}$ is a symmetric tensor and can be diagonalized in the body-fixed principal axes of the polarizability tensor. The polarizability tensor can then be written in Oxyz as

$$\begin{aligned} \overleftrightarrow{\alpha} =& \alpha_{XX}\boldsymbol{i}'\boldsymbol{i}' + \alpha_{YY}\boldsymbol{j}'\boldsymbol{j}' + \alpha_{ZZ}\boldsymbol{k}'\boldsymbol{k}' + \alpha_{XY}(\boldsymbol{i}'\boldsymbol{j}' + \boldsymbol{j}'\boldsymbol{i}') + \alpha_{YZ}(\boldsymbol{j}'\boldsymbol{k}' + \boldsymbol{k}'\boldsymbol{j}') \\ &+ \alpha_{ZX}(\boldsymbol{k}'\boldsymbol{i}' + \boldsymbol{i}'\boldsymbol{k}') \end{aligned} \tag{6.23}$$

Table 6.2 Spherical components of symmetric polarizability tensor fixed to a particle

$\alpha_0^{(0)} = (1/\sqrt{3})(\alpha_{XX} + \alpha_{YY} + \alpha_{ZZ})$
$\alpha_0^{(2)} = (1/\sqrt{6})[3\alpha_{ZZ} - (\alpha_{XX} + \alpha_{YY} + \alpha_{ZZ})]$
$\alpha_{\pm 1}^{(2)} = \pm(\alpha_{ZX} \pm i\alpha_{YZ})$
$\alpha_{\pm 2}^{(2)} = (1/2)[\alpha_{XX} - \alpha_{YY}) \pm i2\alpha_{XY}]$

where the six components, α_{XX}, $\alpha_{YY}, \ldots,$ are independent and $\boldsymbol{i}'$, $\boldsymbol{j}'$, and $\boldsymbol{k}'$ are unit vectors along the X, Y, and Z axis, respectively. If the particle rotates in space (Oxyz), these unit vectors rotate with it and the components of $\overleftrightarrow{\boldsymbol{\alpha}}$ along space-fixed coordinates change their values in time. The transformation law of the polarizability is similar to that of the products of coordinates, XX, $XY, \ldots$. We have seen in Table 4.2 that linear combinations of x^2, $xy, \ldots$ form a set of five spherical harmonics of order 2, which is convenient to be used for characterizing rotations of an ellipsoid of rotation. There is another independent linear combination, $x^2+y^2+z^2$, which is invariant under rotation (Exercise 6.17). Thus, we have altogether six linear combinations. The polarizability tensor has also six linearly independent component and its rotation in the Oxyz system can be characterized by the similar combinations of XX, $XY, \ldots$. These are listed in Table 6.2.

When the particle rotates, the spherical components mix each other among $\alpha_{\mathrm{m}}^{(j)}$ within the group of the same order j. This is an advantage of using the spherical components. Namely, we have

$$\alpha_{\mathrm{m}}^{(2)}(L,t) = \sum_{\mathrm{m}'} \alpha_{\mathrm{m}'}^{(2)}(B) R_{\mathrm{m}'\mathrm{m}}^{(2)}(\alpha,\beta,\gamma,t) \tag{6.24}$$

where $R_{\mathrm{m}'\mathrm{m}}^{(2)}$ is the rotation matrix (Edmunds, 1957) and α, β, and γ are the Euler angles at t. The rotation matrix is closely related to the eigenfunctions $D_{\mathrm{m,M}}^{(2)}$ of Eqs. 4.56, 4.57, and 4.58. The relation is given by

$$R_{\mathrm{m}'\mathrm{m}}^{(J)}(\alpha,\beta,\gamma,t) = [8\pi^2/(2J+1)]^{1/2} D_{\mathrm{m}'\mathrm{m}}^{(J)}(\alpha,\beta,\gamma,t) \tag{6.25}$$

so that Eq. 6.24 can be rewritten as

$$\alpha_{\mathrm{m}}^{(2)}(L,t) = [8\pi^2/5]^{1/2} \sum_{\mathrm{m}'} \alpha_{\mathrm{m}'}^{(2)}(B) D_{\mathrm{m}'\mathrm{m}}^{(2)}[\alpha,\beta,\gamma,t) \tag{6.26}$$

The arguments, L and B, stand for the laboratory and body system, respectively. Now we can find how the rotation affects the scattering.

In light scattering, suppose that the incident light is polarized vertically in the z direction in the laboratory system. The scattered light may be observed with the

Table 6.3 Polarizability tensor in the true symmetric top case ($\alpha_{XX}(B) = \alpha_{YY}(B) \equiv \alpha_\perp$, $\alpha_{ZZ}(B) = \alpha_\parallel$)

$\alpha_0^{(0)}(B) = (1/\sqrt{3})(2\alpha_\perp + \alpha_\parallel)$
$\alpha_0^{(2)}(B) = 2/\sqrt{6}[\alpha_\parallel - \alpha_\perp]$
$\alpha_{\pm1}^{(2)}(B) = \alpha_{\pm2}^{(2)}(B) = 0$

same vertical polarization or the horizontal polarization (y direction). In this configuration, the incident light is in the xy plane (the scattered light is in the x direction). Then, the components of the polarizability important for these scattering are, in the laboratory system, α_{zz} and α_{zy}, which can be written in terms of spherical components by solving the relations of Table 6.2 written in the laboratory system as

$$\text{Vertical-Vertical}: \qquad \alpha_{zz} = (1\sqrt{3})\alpha_0^{(0)}(L) + \sqrt{(2/3)}\alpha_0^{(2)}(L) \tag{6.27}$$

$$\text{Vertical-Horizontal}: \qquad \alpha_{zy} = -(\mathrm{i}/2)[\alpha_1^{(2)}(L) + \alpha_{-1}^{(2)}(L)] \tag{6.28}$$

The right hand sides must be written in terms of the body-fixed components by means of Eq. 6.26, so that we can take averages over the Brownian rotation of the body-fixed quantities by using Eq. 4.64.

For simplicity, assume that our Brownian particles are of a symmetric top and the principal axes of the polarizability tensor and the rotational diffusion tensor coincide (a true symmetric top case). The spherical components of $\overleftrightarrow{\boldsymbol{\alpha}}$ in the Oxyz system is given in Table 6.3.

Note that the number of the independent components is the same in either the Cartesian or the spherical representation. Thus, the reduced amplitudes of the scattered electric fields are given by

$$\boldsymbol{E}_{VV}(t) = \alpha_{zz}(t)\boldsymbol{E}_i/E_i^0 = [(1/\sqrt{3})\alpha_0^{(0)} + \sqrt{(16\pi^2/15)}\alpha_0^{(2)}(B)D_{0,0}^{(2)}(\Omega, t)$$

$$\boldsymbol{E}_{VH}(t) = \alpha_{yz}(t)\boldsymbol{E}_i/E_i^0 = -i\sqrt{(4\pi^2/10)}\alpha_0^{(2)}(B)[D_{0,1}^{(2)}(\Omega, t) + D_{0,-1}^{(2)}(\Omega, t)]$$

where $\Omega = (\alpha, \beta, \gamma)$.

The correlation functions of the amplitudes can be obtained by averaging over the rotational Brownian motion by means of Eq. 4.64. The averages are taken on both distributions of the initial Ω_0 at $t=0$ and the final Ω at $t=\tau$ by using Eq. 4.60. The results are given by

$$\langle \boldsymbol{E}_{VV}(\tau) \cdot \boldsymbol{E}_{VV}(0) \rangle = \frac{1}{9}(\boldsymbol{\alpha}_\parallel + 2\boldsymbol{\alpha}_\perp)^2 + \frac{4}{45}(\boldsymbol{\alpha}_\parallel - \boldsymbol{\alpha}_\perp)^2 \mathrm{e}^{-6D_\perp^r \tau} \tag{6.29}$$

$$\langle \boldsymbol{E}_{VH}(\tau) \cdot \boldsymbol{E}_{VH}(0) \rangle = \frac{1}{15} (\boldsymbol{\alpha}_{\parallel} - \boldsymbol{\alpha}_{\perp})^2 \mathrm{e}^{-6D^{\mathrm{r}}_{\perp}\tau} \tag{6.30}$$

Finally, for monodisperse systems, including the translational part of the correlation function, the autocorrelation function for a true symmetry top case is given by the product of Eq. 6.22 and Eq. 6.29 for $\psi_{\mathrm{VV}}(\tau)$ or that of Eq. 6.22 and Eq. 6.30 for $\psi_{\mathrm{VH}}(\tau)$.

$$\psi_{VV}(\tau) = \frac{1}{9} (\boldsymbol{\alpha}_{\parallel} + 2\boldsymbol{\alpha}_{\perp})^2 \mathrm{e}^{-q^2 Dt} + \frac{4}{45} (\boldsymbol{\alpha}_{\parallel} - \boldsymbol{\alpha}_{\perp})^2 \mathrm{e}^{-(q^2 D + 6D^{\mathrm{r}}_{\perp})\tau} \tag{6.31}$$

$$\psi_{VH} = \frac{1}{15} (\boldsymbol{\alpha}_{\parallel} - \boldsymbol{\alpha}_{\perp})^2 \mathrm{e}^{-(q^2 D + 6D^{\mathrm{r}}_{\perp})\tau} \tag{6.32}$$

The frequency distribution is given by taking the Fourier transform of these correlation functions (see Eq. 6.20). When N particles are in the scattering volume, we have

$$I_{VV}(q, \Delta\omega) = \langle N \rangle \frac{1}{\pi} \left[\frac{1}{9} (\boldsymbol{\alpha}_{\parallel} + 2\boldsymbol{\alpha}_{\perp})^2 \frac{q^2 D}{\Delta\omega^2 + (q^2 D)^2} + \frac{4}{45} (\boldsymbol{\alpha}_{\parallel} - \boldsymbol{\alpha}_{\perp})^2 \frac{6D^{\mathrm{r}}_{\perp} + q^2 D}{\Delta\omega^2 + (6D^{\mathrm{r}}_{\perp} + q^2 D)^2} \right] \tag{6.33}$$

$$I_{VH}(q, \Delta\omega) = \langle N \rangle \frac{1}{\pi} \frac{(\boldsymbol{\alpha}_{\parallel} - \boldsymbol{\alpha}_{\perp})^2}{15} \frac{6D^{\mathrm{r}}_{\perp} + q^2 D}{\Delta\omega^2 + (6D^{\mathrm{r}}_{\perp} + q^2 D)^2} \tag{6.34}$$

For polydisperse systems, these expressions are very complicated.

The first term of ψ_{VV} (Eq. 6.31) or I_{VV} (Eq. 6.33) may be obtained with the help of the experimental result of ψ_{VH} or I_{VH} . Thus, we find the value of D. Then, $D^{\mathrm{r}}_{\perp}$ can be determined from the above equations.

The diffusion coefficient of a spherical particle of radius of 100 nm in water at 25°C is about $2.4 \cdot 10^{-12}$ m^2/s. If $\lambda = 500$ nm in water and $\theta = 90°$, $q = 1.8 \cdot 10^7$/m and $q^2 D = 758$/s. This frequency shift is too small to be optically observed by using a diffraction grating or an interferometer (called as a filter method). This optical method is feasible if the dynamic scattering process is faster than 10^{-6} s. If the process is slower, a photomultiplier may be used. A good photomultiplier has a time resolution of about 10^{-11} s and in order to extract the slow signal due to Brownian motion from the output it may be necessary to lower the frequency of the signal by beating it with itself through time delay or with a light wave of another local oscillator. We know that the beat frequency of two waves, ω_1 and ω_2, is $\omega_1 - \omega_2$. Although the output of a photomultiplier is photoelectrons or a photocurrent, we can use a correlation method on the output to see the beating process.

6.2.2.3 Photon Correlation in Slightly Dense Monodisperse Systems

In Sec. 6.2.2.2, we have assumed that particles independently scatter the incident light. But, when the concentration increases or interparticle interactions cannot be ignored, the correlation between the fields scattered by different particles must be included in the treatment. The general form of the autocorrelation function, Eq. 6.21, can be written in terms of the dynamic structure factor define by

$$F(q,\tau) = \frac{1}{N\langle f^2(q)\rangle}\sum_j \sum_{j'} \left\langle f_j(q,\tau+t_0) f_{j'}(q,t_0) \mathrm{e}^{i\boldsymbol{q}\cdot(\boldsymbol{x}_j(\tau+t_0)-\boldsymbol{x}_{j'}(t_0))} \right\rangle \quad (6.35)$$

where j and j' refer to the j-th and j'-th particle, respectively, and f_j is the amplitude of the scattered field by the j-th particle. The average, $\langle\ \rangle$, implies, as in Eq. 6.21, that it is taken with respect to t_0. Statistically, however, it is equivalent to take the average over the all possible positions and orientations of the particles at $t=0$. The summations over j and j' imply then the same average over t_0. We can therefore omit the symbol, $\langle\ \rangle$, in Eq. 6.35 and set $t_0=0$. The Fourier transform of Eq. 6.35 with respect to τ gives the line broadening, Eq. 6.20.

If the particles are nonspherical, the amplitude also undergoes the Brownian motion independent from or coupled with the translational motion. The scattered intensity depends on the square of the particle volume (in the Rayleigh regime). This size effect also makes the dynamic structure factor complicated for polydisperse systems.

If particles are spherical in monodisperse systems, the average in Eq. 6.35 can be simplified and we have

$$F(g,\tau) = \frac{1}{N}\sum_j \sum_{j'} \mathrm{e}^{i\boldsymbol{q}\cdot(\boldsymbol{x}_j(\tau)-\boldsymbol{x}_{j'}(0))} = F_\mathrm{s}(q,\tau) + \frac{1}{N}\sum_j \sum_{\neq j'} \mathrm{e}^{i\boldsymbol{q}\cdot(\boldsymbol{x}_j(\tau)-\boldsymbol{x}_{j'}(0))} \quad (6.36)$$

Here, $F_\mathrm{s}(q,\tau)$ is the self-dynamic structure factor:

$$F_\mathrm{s}(q,\tau) = \left\langle \mathrm{e}^{i\boldsymbol{q}\cdot(\boldsymbol{x}(\tau)-\boldsymbol{x}(0))} \right\rangle \quad (6.37)$$

In Eq. 3.36, for large q, each of the second term oscillates very rapidly and vanishes on the average over the distribution, say, j', so that

$$F(q,\tau) \to F_\mathrm{s}(q,\tau)\ , \quad \text{as} \quad q \to \infty \quad (6.38)$$

Particles then behave independently and the self-diffusion coefficient may be given by the behavior for the large q regime. However, as we have seen at Eq. 4.28, the large q corresponds to short times. The diffusion coefficient given by Brownian motion, Eq. 4.19, is associated with the long times, corresponding to a small q.

For the small q regime, which corresponds to $t \to \infty$, we can assume that the system approaches a stationary state. Rewriting $F(q,\tau)$

$$F(q,\tau) = \frac{1}{N}\sum_j \sum_{j'} \mathrm{e}^{i\boldsymbol{q}\cdot(\boldsymbol{x}_j(\tau)-\boldsymbol{x}_j(0)+\boldsymbol{x}_j(0)-\boldsymbol{x}_{j'}(0))}$$

If $\exp(i\boldsymbol{q}\cdot(\boldsymbol{x}_j(\tau)-\boldsymbol{x}_j(0))$ can be assumed to be independent from the remaining factor at long times, we have

$$F(q,\tau) = F(q,0)\mathrm{e}^{-D_c q^2 \tau} \tag{6.39}$$

where D_c is called the collective diffusion coefficient ($D_c = D/F(q,0)$). The factor $F(q,0)$ is the static structure factor and is known to be related to the isothermal osmotic compressibility through (Vrij et al., 1978)

$$F(q,0) = k_B T\left(\frac{\partial n}{\partial \Pi}\right)_T \tag{6.40}$$

where Π is the osmotic pressure and n is the particle number density.

Therefore, in monodisperse systems, when particles are subject to interparticle interactions, the autocorrelation function of Eq. 6.22 is replaced by

$$\Psi(q,\tau) = k_B T\left(\frac{\mathrm{d}n}{\mathrm{d}\Pi}\right)_T \mathrm{e}^{-D_c q^2 \tau} \tag{6.41}$$

6.2.2.4 Higher-order Correlation Functions

The correlation functions, Eqs. 6.22, and 6.29-32, in Sec. 6.2.2, are of the first order. Experimentally, such correlations do not directly appear in the output of a photomultiplier or a photo- sensitive solid-state device, unless a correlation of the outputs at different times, t and $t+\tau$ (τ: delay parameter), is taken with a running time t. Thus, it requires, at least, the second-order correlation functions $\langle i((t)\, i(t+\tau)\rangle \propto \langle E^*(t)E(t)E^*(t+\tau)E(t+\tau)\rangle$, where $i(t)$ and $i(t+\tau)$ are output of the electronic detector. Such correlations can be computed electronically on a computer (a correlator). This method is applicable if the dynamic scattering process is slower than 10^{-6} s. There are various modifications as described below, including a mixing of the scattered light and a light beam from a local oscillator.

In photodetection, the number of photons are counted. Then the wave representing the photons cannot have a definite phase. From the uncertain relation, $\Delta E \cdot \Delta t \sim \hbar$, ($\hbar$: Planck's constant/$2\pi$), we have, since $\Delta E = \hbar\omega\Delta n$ (n: number of photons) and $\Delta(\omega t) = \Delta\phi$ (ϕ: phase),

$$\Delta n \cdot \Delta\phi \sim 1 \tag{6.42}$$

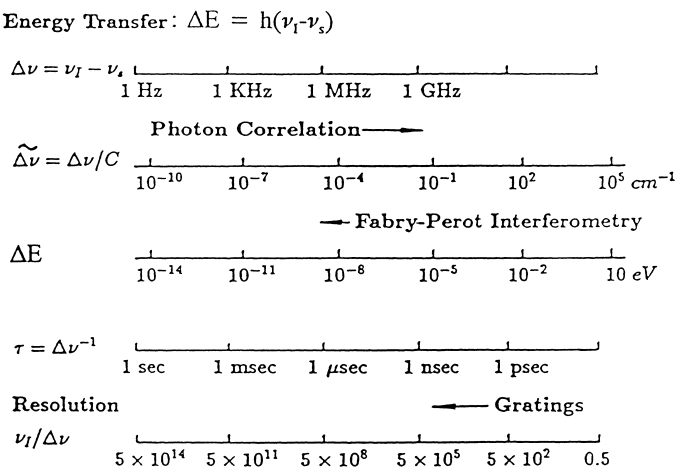

Fig. 6.3 Line width and applicability of photon correlation spectroscopy, Fabry-Perot interferometry, and grating spectroscopy. The ends of the arrows suggest approximate limits of applicability (Chu, 1991, with permission from Academic Press).

Thus, the intensity measured by photoelectric emission is the cycle-averaged intensity. We note that the cycle-averaged quantities can be easily obtained from Eq. 6.14 by taking a half of the product of the field and its complex conjugate (see Jackson, 1975, p. 241). We must remember that the magnetic part of the wave also contributes to the intensity by the equal amount.

The simplest second-order photon correlation spectroscopic methods are the following three (Chu, 1991).

A) Self-beating method. The output of a photomultiplier (PM tube), which receives a scattered light, is sampled at t and $t+\tau$ (t: running time, τ: an adjustable parameter) with a fixed sampling time T. The two sampled signals are numerically multiplied (mixed), and the product is averaged over the running time. The beat frequency here is zero.

The output, a photocurrent i or a number n of photoelectrons during a short sampling time T is proportional to the intensity and we can compute the second-order correlation function by

$$\langle i(t)i(t+\tau)\rangle \propto \langle n(t)n(t+\tau)\rangle/T^2 \propto \langle I(t)I(t+\tau)\rangle \tag{6.43}$$

Now $I(t) \propto |E(t)|^2$ with $E(t)=\sum_k E_k \exp[-i\phi_k(t)]$ at the photocathode, where the subscript k refers to the k-th particle producing a random phase ϕ_k by Brownian motion. Here, we assume that E_k is constant. Using this $E(t)$, we have

$$\langle i(t)i(t+\tau)\rangle \propto \sum_{k_1k_2k_3k_4} \langle E_{k_1}^* E_{k_2}^* E_{k_3} E_{k_4} e^{i[\phi_{k_1}(t)+\phi_{k_2}(t+\tau)-\phi_{k_3}(t+\tau)-\phi_{k_4}(t)]}\rangle \tag{6.44}$$

Noting that the phases are random variables, there are only two types of the following terms in the summation for which the ensemble averages do not vanish.

$$k_1 = k_4\ ,\quad k_2 = k_3 \quad \text{and} \quad k_1 = k_3\ ,\quad k_2 = k_4 \tag{6.45}$$

If the scattering volume contains a very large number of Brownian particles, Eq. 6.44 leads to

$$\langle i(t)i(t+\tau)\rangle \propto \langle E^*(t)E(t)\rangle^2 + |\langle E^*(t)E(t+\tau)\rangle|^2 \tag{6.46}$$

Therefore, if we define the normalized first-order and second- order correlation function by

$$g^{(1)}(\tau) = \langle E^*(t)E(t+\tau)\rangle / \langle E^*(t)E(t)\rangle \tag{6.47}$$

$$g^{(2)}(\tau) = \langle i(t)i(t+\tau)\rangle / \langle i^2(t)\rangle \tag{6.48}$$

respectively, we have

$$g^{(2)}(\tau) = 1 + |g^{(1)}(\tau)|^2\ , \quad (\tau \not\simeq 0) \tag{6.49}$$

From this equation $|g^{(1)}(\tau)|$ can be obtained if $g^{(2)}(\tau)$ is known.

Equation 6.49 is valid only for a short sampling time ($T \ll$ correlation time, τ_c, ($g^{(1)}(\tau_c) = 1/e$), and the detector size of about the coherent area (Eq. 6.15). Because of the above condition of the large number of particles used in deriving Eq. 6.48, the statistics holding here is Gaussian. The Gaussian distribution is completely determined by its first moment (average) and the second moment (variance). The first-order correlation function is the second moment and the second-order correlation function is the fourth moment. Therefore, they must be related if Gaussian statistics is applicable.

B) Homodyne method. A scattered light, $E_s(t)$, and the field, $E_{LO}(t)$, of a local oscillator of the same frequency, ω_0, as the incident illuminate the photocathode. Then, those waves are mixed at the detector and $E(t) = E_s(t) + E_{LO}\exp(-i\omega_0 t)$, which is used in Eq. 6.46.

C) Heterodyne method. A small portion of the unscattered light (local oscillator) of a different frequency is mixed with the scattered light at the photocathode. Thus,

$$E(t) = E_s(t) + E_{LO}\exp(-i\omega_{LO}t) \tag{6.50}$$

where E_s is the scattered light expressed by $\sum_k E_k \exp[-i\phi_k(t)]$ and the local oscillator is assumed not to fluctuate. Substituting this into Eq. 6.46, we have the second-order correlation function. However, we choose the experimental conditions,

such that the amplitude of the local oscillator is much greater than the amplitude of the scattered field. Therefore, in the second-order correlation function, the terms which do not contain the local oscillator field, E_{LO}, may be ignored. Then, we have

$$\langle i(t)i(t+\tau)\rangle \propto |E_{LO}|^4 + 2|E_{LO}|^2\langle E_s^*(t)E_s(t+\tau)\rangle \tag{6.51}$$

The last term is complex if there is a flow of scattering particles as a whole. Then, take the real part.

6.3 Small-angle X-Ray Scattering

The wavelength of an x-ray is about 0.1 nm and the scattering essentially occurs by electrons. If the x-ray photon energy is much larger than the binding energy of an electron, the electron may behave like a free electron. In the limiting case of the Compton scattering, Thompson classically considered that, when an x-ray irradiated such an electron, it started to oscillate almost freely and emitted a coherent scattered x-ray. Since an atomic nucleus is much heavier than an electron, it can hardly move under x-rays and has a much less scattering power. In fact, the scattering cross-section is inversely proportional to the square of the mass of the particle. The x-rays can be produced by bombarding a high-energy electron beam on a metallic target in vacuum. Recently, synchrotron radiation sources are also becoming widely available with possibilities of longer wavelengths.

X-rays can be used to investigate electronic structures in small particles of size of down to a few nm. It is particularly useful in structural study of micelles, microemulsions, clusters, etc. (J. Physique IV, Colloque C8, 1993).

We have seen in Sec. 6.2.1 that if the particle size is large compared with the wavelength, λ, the forward scattering is predominant. Because of this small-angle scattering is important in x-rays. (For example, in the study of a crystal structure of a spacing of 10 nm with Cu K_α radiation (λ: 0.15 nm), the diffraction angle is 0.86°.) The scattered x-ray wave from a single electron can also be expressed by Eq. 6.8 or 6.13, where $\boldsymbol{q}=(2\pi/\lambda)$ $(\boldsymbol{n}_s-\boldsymbol{n}_0)$ with (the refractive index of x-rays is nearly unity)

$$q = \frac{4\pi \sin(\theta/2)}{\lambda} \tag{6.52}$$

If we can ignore the effects of multiple scattering, the scattered intensity from a particle is then given by

$$I(q) = I_e\left|\sum_j f_j e^{i\boldsymbol{q}\cdot\boldsymbol{x}_j}\right|^2 = I_e F(q) \tag{6.53}$$

Here f_j is the scattering factor of the j-th electron in the particle and $F(q)$ is the structure factor. When $f_j = 1$ for all j, $F(q)$ is listed for various shapes in Table 6.1, assuming a uniform electronic distribution within the shape. But note that $F(q)$ of Eq. 6.9 is normalized per particle, while the above $F(q)$ is not normalized per electron. However, remember that the above $I(q)$ is expressed per particle. I_e is the scattered intensity by a single electron and depends on q, given by

$$I_e(q) = 7.90 \cdot 10^{-28} I_0 R^{-2} (1 + \cos^2 \theta)/2$$

where I_0 is the intensity of the incident beam and R is the distance from the observer, expressed in meters. Note, however, that $\cos\theta$ is almost unity for small angles and the dependence of I_e on q can be ignored.

As given by Eq. 6.12, the concept of a radius of gyration a_G and Table 4.1 may be used. Assuming that the particle has a center of symmetry, we choose the origin of the coordinates at the center. Since the term $2\boldsymbol{x}_j \cdot \boldsymbol{x}_{j'}$, in $r_{jj'}^2 = |\boldsymbol{x}_j - \boldsymbol{x}_{j'}|^2 = \boldsymbol{x}_j^2 + x_{j'}^2 - 2\boldsymbol{x}_j \cdot \boldsymbol{x}_{j'}$ vanishes because of the symmetry on summation over j and j', we can write

$$a_G = \left(\sum_j f_j \boldsymbol{x}_j^2 \right) \Big/ \sum_j f_j \tag{6.54}$$

where a_G is the radius of gyration. Hence, the scattered intensity by the particle is given by

$$I(q) = I_e \left(\sum_j f_j \right)^2 [1 - (q a_G)^2/3 + \cdots] = I_e N_e^2 \exp(-(q a_G)^2/3) \tag{6.55}$$

where $N_e = \sum_j f_j$, the total number of electrons in the particle.

In handling Eq. 6.53, we can consider that electrons belong to atoms in a particle, unles it is metallic. We can then refer the equation to the j-th atom instead of the j-th electron and f_j can be considered as the scattering factor for this atom. This atomic f_j behaves, again, as a constant for small angles.

In a scattering volume of N particles, since the scattering cross-section of a single electron is very small, we can assume that the multiple scattering is less probable and we simply sum scattered waves over all their electrons. For simplicity, we assume that the particles are identical. If the particles are oriented in the same direction, their structure factors are the same. But they are in motion in solution and we must average over their orientations. In the k-th particle, the position of the scattering electron, j, is defined by $\boldsymbol{x}_{kj} + \boldsymbol{R}_k$, where $\boldsymbol{x}_{kj}$ is the radial vector from the center of mass at $\boldsymbol{R}_k$ of particle k. Then, the sum can be written as

$$I(q) = I_e \left\langle \left| \sum_k \sum_j f_{kj} e^{i(\boldsymbol{q} \cdot (\boldsymbol{x}_{kj} + \boldsymbol{R}_k))} \right|^2 \right\rangle \tag{6.56}$$

The symbol, $\langle\ \rangle$, designates the average over orientations and positions. Note that $\boldsymbol{x}_{kj}$ is the relative position of the j-th electron within the k-th particle. We can separate $\boldsymbol{x}_{kj}$ and $\boldsymbol{R}_k$:

$$I(q) = I_e \left\langle \sum_k \sum_{k'} \left[\sum_j f_{kj} e^{-i\boldsymbol{q}\cdot\boldsymbol{x}_{kj}} \right] \left[\sum_{j'} f_{k'j'} e^{i\boldsymbol{q}\cdot\boldsymbol{x}_{k'j'}} \right] e^{i\boldsymbol{q}\cdot(-\boldsymbol{R}_k+\boldsymbol{R}_{k'})} \right\rangle \tag{6.57}$$

Note that, for the term $k=k'$, the two factors of square brackets are the same, but, for $k \neq k'$, they belong to different particles and are independent in their motion and must be individually averaged. Thus, noting $F(q)$ given by Eq. 6.53, we can write

$$I(q) = I_e \left[N \cdot F(q) + \left| \left\langle \sum_j f_j e^{i\boldsymbol{q}\cdot\boldsymbol{x}_j} \right\rangle \right|^2 \left\langle \sum_k \sum_{\neq k'} e^{-i\boldsymbol{q}\cdot(\boldsymbol{R}_k-\boldsymbol{R}_{k'})} \right\rangle \right] \tag{6.58}$$

If we denote by $p(|\boldsymbol{R}_k - \boldsymbol{R}_{k'}|)\mathrm{d}V_k \mathrm{d}V_{k'}/V_0^2$ the probability of finding the k-th particle in $\mathrm{d}V_k$ and the k'-th particle in $\mathrm{d}V_{k'}$ $(k \neq k')$, where V_0 is the average volume offered to each particle $(V_0 = V/N)$, by using the approximation, Eq. 6.11, we have

$$\left\langle \sum_k \sum_{\neq k'} e^{i\boldsymbol{q}\cdot(\boldsymbol{R}_k-\boldsymbol{R}_{k'})} \right\rangle = \frac{1}{2} \int_V \int_V \frac{\sin(qR_{kk'})}{qR_{kk'}} p(R_{kk'}) \frac{\mathrm{d}V_k}{V_0} \frac{\mathrm{d}V_{k'}}{V_0} ,$$
$$R_{kk'} = |\boldsymbol{R}_k - \boldsymbol{R}_{k'}| \tag{6.59}$$

In Eq. 6.59, if $p(R_{kk'}) = 1$, the particles are uniformly distributed in the scattering volume V and V is of the order of 1 mm^3, so that Eq. 6.59 almost vanishes except for the very sharp forward direction. Namely, this term cannot be observed if $p(R_{kk'}) = 1$. Thus, we can rewrite the expression as

$$\left\langle \sum_k \sum_{\neq k'} e^{i\boldsymbol{q}\cdot(\boldsymbol{R}_k-\boldsymbol{R}_{k'})} \right\rangle = -\frac{1}{2} \int_V \int_V \frac{\sin(qR_{kk'})}{qR_{kk'}} [1 - p(R_{kk'})] \frac{\mathrm{d}V_k}{V_0} \frac{\mathrm{d}V_{k'}}{V_0} \tag{6.60}$$

If the distance $R_{kk'}$ is small, the detailed distribution is important. But if it is large we can treat the average distribution, so that $p(R_{kk'})$ is close to unity for large distances. Therefore, $1 - p(R_{kk'})$ vanishes for large distances, implying the integration limits can be extended. We have

$$\left\langle \sum_k \sum_{\neq k'} e^{i\boldsymbol{q}\cdot(\boldsymbol{R}_k-\boldsymbol{R}_{k'})} \right\rangle = -\int_V \frac{\mathrm{d}V_{k'}}{V_0} \int_0^\infty \frac{\sin(qR)}{qR} [1 - p(R)] \frac{2\pi R^2 \mathrm{d}R}{V_0} \tag{6.61}$$

Since $\int_V \mathrm{d}V_{k'}/V_0 = N$, the number of particles, we can finally write

$$I(q) = N \cdot I_e \left[F(q) - \frac{\left| \left\langle \sum_j f_j e^{i\boldsymbol{q}\cdot\boldsymbol{x}_j} \right\rangle \right|^2}{V_0} \int_0^\infty \frac{\sin(qR)}{qR} [1 - p(R)] 2\pi R^2 \mathrm{d}R \right] \tag{6.62}$$

The last term of Eq. 6.62 is due to interparticle interferences. It is small if the dispersion is dilute or random and it can then be ignored.

The similar scattering occurs due to electrons of the solvent. Thus, the total scattering from the system must include the solvent. The contribution comes from the solvent excluded in volume by the particles and is given by

$$\rho_s \left[\int_{\text{whole volume}} \mathrm{d}V_s f_s e^{i\boldsymbol{q}\cdot\boldsymbol{x}_s} - N \int_{V_0} \mathrm{d}V_s f_s e^{i\boldsymbol{q}\cdot\boldsymbol{x}_s} \right]$$

where ρ_s is the averaged number density of electrons in the solvent, $\boldsymbol{x}_s$ is the position vector of the s-th electron in the solvent, and V_0 is the volume of the particle. The first integral is over the whole target volume. In the limit of a bulk sample, this integral approximates a delta function $\delta(\boldsymbol{q})$, which is zero for $\boldsymbol{q} \neq 0$. Hence this term does not contribute to the scattering. Therefore, the scattered intensity from the dilute solution of the particles in the solvent is given by (no interparticle interference)

$$I(q) = KN \cdot I_e [(\rho_p - \rho_s)/\rho_p]^2 F(q), \tag{6.63}$$

where K is the instrumental correction factor and ρ_p is the averaged electronic number densities in the particle. Hence, it is desirable that the electronic density of the solvent be as much different as possible from that of the particles.

The zero-angle intensity $I(0)$ can be obtained by an extrapolation of an experimental plot of $\ln [I(q)]$ against q^2. This is because from Eqs. 6.55 and 6.63 we have

$$\ln I(q) = \ln I(0) - (a_G q)^2/3$$

Since $I(0) = KN \cdot I_e [(\rho_p - \rho_s) V_0]^2$, we find the number of electrons in the particle if we know ρ_s from a knowledge of the solvent. The slope of the plot gives the value of a_G and accordingly the particle size (Kratky and Glatter, 1982). This plot is called the Guinier plot (Guinier, 1939). This plot is usually useful for small values of q ($a_G q < 1$). For larger values of q, $\ln I(q)$ may be plotted against q, showing an undulatory behavior with pronounced peaks dependent on the particle radius. These peaks are not due to the interference of x-rays scattered by different

particles and they are smoothed out in polydisperse systems (Hashimoto et al., 1980).

If the electron density is not uniform in a particle, $I(q)$ can also have peaks at various values of q. An example is a micelle, which has a hydrophobic core and a hydrophilic shell. The two regions have distinct electronic densities. In such a core-shell structure, a strong scattering peak can sometimes appear due to the interference. Such a peak does not depend on the concentrations of the particle in a solution and can be easily recognized (Zemb and Charpin, 1985). The structure can only be determined by finding a theoretical structure to which the experimental $I(q)$ fits well (Friman and Rosenholm, 1982; Chen et al., 1977; Marignan et al., 1986; Matsuoka et al., 1988).

Since the wavelength of an x-ray can be comparable with the size of particle clusters or aggregates in disperse systems, the small angle scattering may be used for investigating their structure. (Light and neutron scattering may also be used.) Consider an aggregate of identical particles of size a. For $q \gg 1/a_G$, where a_G is the radius of gyration of the aggregate, as shwon below, $I(q)$ depends on the shape of the particle and satisfies (Fig. 5.4)

$$I(q) = I_e P q^{-x}, \quad (P: \text{ constant}) \tag{6.64}$$

If the aggregate is a straight linear cluster of particles (randomly oriented), $x=1$. If it is, instead, a very thin, circular disc, $x=2$.

The power law of Eq. 6.64 suggests a fractal structure within a certain range of q (see Sec. 5.4). In practical cases, because of the roughness of the surface and the flexibility of the shape of the aggregate, the value of the exponent x differs from the above values of ideal cases. In general, a convenient plot for obtaining the value of x in experiments is a $\ln I(q)$–$\ln q$ plot. The application of the x-ray scattering to fractal structures is discussed by Schmidt (1989).

The scattered intensity $I(q)$ from a randomly oriented aggregate of N identical, rigid, spherically symmetric, uniform particles of diameter a, averaged over all orientations of the aggregate, is given by the equation (see Eq. 6.62):

$$I(q) = N I_e F_a(q) S(q) \tag{6.64a}$$

where $I_e F_a(q)$ is the scattered intensity from one constituent particle of radius a ($F(q)$ in Eq. 6.53) and

$$S(q) = 1 + 4\pi \frac{N}{V} \int_a^l r^2 g(r) \frac{\sin qr}{qr} \mathrm{d}r \tag{6.64b}$$

where l is the largest value of the distances between the centers of any pair of constituent particles of the aggregate and $g(r)$ is the normalized distribution function of the particles (strictly speaking, the correlation function, see Chapt. 13). If the aggregate is a fractal which satisfies the power law for small r (fractals being

defined by a limiting process as $r \to 0$, Sec. 5.2), $g(r)$ may be considered as an averaged number density:

$$g(r) = g_0 f(r/l) r^D / r^3 \tag{6.64c}$$

where g_0 is a constant and D is the fractal dimension. The quantity, $f(r/l)\, r^D$, is proportional to the number of particles in the Euclidean three-dimensional volume, which is proportional to r^3. When $r/l \ll 1$, $g(r)$ approaches the fractal limit (r^{D-3}) and $f(r/l) \to 1$. In this limit, we can write Eq. 6.64b as

$$S(q) = 1 + 4\pi \frac{N}{V} g_0 q^{-D} \int_{qa}^{ql} x^{D-1} \frac{\sin x}{x} \mathrm{d}x$$

If $qa \ll 1$, $I_e F_a(q) \to N_e^2 I_e$. Therefore, the q-dependence of $I(q)$ must come from the second term of $S(q)$, Eq. 6.64b. For $ql \gg 1$ and $qa \ll 1$, the value of the integral is a constant and we find that

$$S(q) \propto q^{-D} \tag{6.64d}$$

Therefore, we have

$$I(q) \propto q^{-D} \tag{6.64e}$$

Since $g(r)$, Eq. 6.64c, is proportional to the mass distribution in the fractal aggregate, D may be called the mass fractal dimension, D_m. Since the aggregate occurs in the three-dimensional Euclidean space, we expect that $1 \le D_m \le 3$.

The mass fractal is also called the volume fractal, the dimension of which is denoted by D_v. Comparing Eq. 6.64 with Eq. 6.64e, we find that x is given by D_m or D_v. This occurs if $1 \le x \le 3$. A disperse system exhibiting this mass fractal is said to include aggregates of linear polymers or small colloidal particles (Schafer, 1989; Nakanishi et al., 1992).

If $qa \gg 1$, $\sin(qr)$ oscillates on performing the integration of Eq. 6.64b, since $qr \ge qa$ in the integrand and the integral almost vanishes. Therefore, we have that $S(q) = 1$ and

$$I(q) = N \cdot I_e F_a(q)\,, \quad \text{if} \quad qa \gg 1 \tag{6.64f}$$

The constituent particles of an aggregate then scatter independently. However, the electronic density changes from that of the aggregate to that of the solvent at the surface of the aggregate and particles at the surface will more strongly scatter x-rays than those inside do. The surface transient region in the electronic density appears to have a structure called the surface fractal (Schmidt, 1989). The q-dependence of $I(q)$ must therefore come from the structure for $q \gg 1/a$. Bale and

Schmidt (1984) consider that the surface of the aggregate has a fractal structure of fractal dimension D_s. X-rays scattered by particles bounded on the fractal boundary surface interfere each other and give

$$I(q) \propto q^{6-D_s} \tag{6.64g}$$

The number 6 in the exponents stands for twice of Euclidean three-dimensionality. Comparing this result with Eq. 6.64, we have that the measured value x is related with D_s as $D_s=6-x$. Since $2<D_s<3$ from the above definition of D_s, if $3<x<4$, the fractal observed in the scattering is the surface fractal.

According to Porod (1951), $x=4$ and, therefore, $D_s=2$ if the surface of a particle is smooth. But, if it has a rough surface, D_s increases and x has a value between 3 and 4 depending on the surface roughness. It may suggest that, if rough, the boundary between the particle and the solvent is not sharp. It is known that, when $x=4$ (a smooth surface), the constant P of Eq. 6.64 is given by $P=2\pi NS(\rho_p-\rho_s)^2$, where S is the particle surface area and N is the number of particles in the scattering volume. From Eq. 6.63, $I(0) = N \cdot I_e[V_p(\rho_p - \rho_s)]^2$ if $K=1$, V_p being the particle volume. Thus, we have

$$P/I(0) = 2\pi S/V_p^2 \tag{6.65}$$

For a spherical particle of radius, a, this ratio is $9/(2a^4)$. Thus, a can be obtained by an experimental observation (Matsuoka et al., 1994).

6.4 Small-angle Neutron Scattering

Just like electrons, neutrons can exhibit a wave property (see Exercise 6.2). Neutrons are generated by nuclear reactions in the nuclear reactor and slowed down by moderators. In small-angle neutron scattering, thermal and cold neutrons are used, providing the wavelength range of 0.1 to 2.0 nm. While x-rays are scattered mainly by electrons, neutrons are scattered by atomic nuclei due to nuclear forces and magnetic moments. The interaction range is very small, as large as about 10^{-5} nm. Thus the scattering centers are well separated and hence multiple scattering effects are less pronounced than x-ray and light. Of course, scattered waves from nuclei interfere with each other. Consequently, very concentrated dispersions of particles can be examined and information about the structure of such systems elucidated. This provides a means of linking microscopic structure to the bulk behavior of materials, e.g. their rheology. Future developments will include the examination of systems under sheared conditions (Ashdown, et al., 1990) and during the application of an electric field (Nierlich et al., 1985). Neutrons are electrically neutral. This, in principle, leads to a method for characterizing non-spherical particles. For applications, see Fontana et al. (1992).

Table 6.4 Coherent Scattering Length of Bound Nuclei in 10^{-6} nm

Nucleus	b
Proton (^{1}H)	–3.741
Deuteron (D=^{2}H)	+6.674
Carbon (^{12}C)	+6.653
Oxygen (^{16}O)	+5.805

For other isotopes, see Lovesey (1984).

Neutron scattering can be treated nearly in the same way as for x-rays. The scattering occurs due to a nuclear and magnetic interaction potential between a neutron and a nucleus. The range of the potential is three orders of magnitude smaller than the de Broglie wavelengths of the neutron normally used in scattering experiments (well under the condition of the Rayleigh scattering of light, Sec. 6.2.1). The interaction potential between a neutron at $\boldsymbol{x}$ and a nucleus at $\boldsymbol{R}$ may therefore be expressed in the form of a delta function:

$$V(\boldsymbol{x}) = (2\pi\hbar^2/m_\mathrm{N})b\delta(\boldsymbol{x}-\boldsymbol{R})$$

where m_N is the mass of a neutron and b designates the magnitude of the potential (attractive if $b<0$ and repulsive if $b>0$).

It is experimentally known that $|b|$ has nearly the same value of about $5{\cdot}10^{-6}$ nm (Lovesey, 1984; Sears, 1992). The typical values are listed in Table 6.4. In general, it is complex, with an imaginary part for absorption. The values of Table 6.4 are averaged values over the possible spin states (see below), leading to coherent neutron scattering in the low energy limits. In this limit, a quantum-mechanical calculation with the above $V(\boldsymbol{x})$ leads to a coherent scattering cross-section $4\pi b^2$ with a scattered wave $b{\cdot}\mathrm{e}^{i\boldsymbol{q}\cdot\boldsymbol{x}}$. Customarily, b is called the scattering length.

The average potential with n nuclei in a particle of volume V is given by

$$\begin{aligned}\langle V(\boldsymbol{x})\rangle &= (1/V)\int V(\boldsymbol{x})\mathrm{d}^3x = \int (2\pi\hbar^2/m_\mathrm{N})\sum_j b_j\delta(\boldsymbol{x}-\boldsymbol{R}_j)\mathrm{d}^3x/V \\ &= (2\pi\hbar^2/m_\mathrm{N})\sum_j b_j/V = (2\pi\hbar^2/m_\mathrm{N})n\langle b\rangle/V\ . \end{aligned} \tag{6.66}$$

Here, $\langle \mathrm{b}\rangle$ implies the averaged value of b over the spin distribution of nuclei in the particle. This averaged value is important in defining the refractive index of a medium for neutrons (Eq. 6.71).

In neutron scattering, complication arises from the fact that the scattering length depends on nuclear spins. The system of a neutron (spin: 1/2) and a nucleus (spin: i) has two possible spin states defined by the total spin $I_\pm = \mathrm{i}\pm(1/2)$

(+: both spins are parallel to each other and –: antiparallel). Each spin state has $2I_{\pm}+1$ substates, arising from the orientation of the total spin in space. When a neutron is scattered by a nucleus, the scattering occurs in anyone of the substates with equal probability. The total number of substates for a neutron and a given nucleus is $2(I_+ + I_-)+2 = 4i+2$. As an example, a proton has spin $i = 1/2$ and the number of parallel spin substates is 3 and that of the antiparallel substate is 1. Hence, when neutrons are scattered by a proton, the parallel case occurs with probability of 3/4 and the antiparallel case 1/4. The scattering length for these substates are $b_+ = 1.08 \cdot 10^{-5}$ nm and $b_- = -4.74 \cdot 10^{-5}$ nm, respectively.

Since the distances between nuclei in a particle are large compared with the range of the nuclear forces between them, the nuclear spins are not correlated. Thus, the way of forming the spin states with the incident neutrons is independent of the positions of the nuclei. Therefore, we can write the structure factor for a particle in the following way,

$$F(q) = \left| \sum_j b_j e^{i\boldsymbol{q}\cdot\boldsymbol{x}_j} \right|^2 = \sum_j \sum_{j'} e^{i\boldsymbol{q}\cdot(\boldsymbol{x}_j - \boldsymbol{x}_{j'})} \langle b_j^* b_{j'} \rangle \tag{6.67}$$

where $\boldsymbol{x}_j$ is the position of the j-th nucleus. There is no correlation between b_j and $b_{j'}$ and $\langle b_j^* b_{j'} \rangle = \langle b_j^* \rangle \langle b_{j'} \rangle = |\langle b \rangle|^2$ if $j \neq j'$. Thus, we have

$$\langle b_j^* b_{j'} \rangle = |\langle b \rangle|^2 + \delta_{j,j'} (\langle |b|^2 \rangle - |\langle b \rangle|^2) \tag{6.68}$$

Therefore, Eq. 6.67 becomes

$$F(q) = |\langle b \rangle|^2 \left| \sum_j e^{i\boldsymbol{q}\cdot\boldsymbol{x}_j} \right|^2 + N(\langle |b|^2 \rangle - |\langle b \rangle|^2) \tag{6.69}$$

The first term corresponds to the coherent scattering and the second the incoherent scattering. We see that the total scattering occurs with strength of $\langle |b|^2 \rangle$.

The values of Table 6.4 are $\langle b \rangle$. For the proton case, with the above mentioned values of b_+ and b_-, we have

$$\langle b \rangle = (3/4) b_+ + (1/4) b_- = -3.75 \cdot 10^{-6} \text{ nm}$$

$$\langle |b|^2 \rangle = (3/4) b_+^2 + (1/4) b_-^2 = 6.49 \cdot 10^{-10} \text{ nm}^2$$

$$\text{The coherent scattering cross-section} = 4\pi |\langle b \rangle|^2 = 1.8 \cdot 10^{-10} \text{ nm}^2 ,$$

$$\text{The total scattering cross-section} = 4\pi \langle |b|^2 \rangle = 81.6 \cdot 10^{-10} \text{ nm}^2 .$$

Thus, the incoherent scattering for protons is very strong compared with the coherent scattering. It makes the angle-independent background scattering strong if protons are involved. Another example for the large difference is vanadium.

The difference for deuterons is small. The deuteron has spin 1 ($i=1$), $b_+ = 9.5 \cdot 10^{-6}$ nm, and $b_- = 1.0 \cdot 10^{-6}$ nm.

$$\langle b \rangle = (4/6)b_+ + (2/6)b_- = 6.7 \cdot 10^{-6} \text{ nm}$$

$$\langle |b|^2 \rangle = (4/6)b_+^2 + (2/6)b_-^2 = 6.1 \cdot 10^{-11} \text{ nm}^2$$

$$\text{The coherent scattering cross-section} = 5.6 \cdot 10^{-10} \text{ nm}^2 ,$$

$$\text{The total scattering cross-section} = 7.7 \cdot 10^{-10} \text{ nm}^2 .$$

Therefore, for deuterons only a relatively small part is incoherent.

Usually, there are many nuclei bound in a molecule or a particle. According to the structure factor, Eq. 6.69, for the coherent scattering part, the average $\langle b \rangle$ over the nuclei in a particle is important in application of neutron scattering. From Eq. 6.66, $\langle b \rangle$ is proportional to the scattering potential averaged over the particle. This quantity $\langle b \rangle$ is usually introduced in terms of the scattering length density, ρ_b, defined for a particle (molecule) of volume, V_0, by

$$\rho_b = \sum_j b_j / V_0 \tag{6.70}$$

This quantity has a similar role in neutron scattering to the electronic density used in x-ray scattering.

As an example of the scattering length density, consider a water molecule, H_2O. Since the density of water is 1 g/cm^3, it is given by

$$[(2 \times (-3.74) + 5.81) \cdot 10^{-13}]/[(2 + 16)/(6.02 \times 10^{23})] \text{ cm}^{-2} = -5.59 \times 10^9 \text{ cm}^{-2} .$$

On the other hand, for D_2O it is 6.34×10^{10} cm^{-2}. It is interesting to note that the values of the scattering length densities of many molecules are between these two values of H_2O and D_2O.

The refractive index for neutron beam can be defined in terms of the averaged quantities, $\langle V(\boldsymbol{x}) \rangle$ or ρ_b, like for light propagating in medium. The de Broglie wavelengths are defined in terms of momenta in the vacuum and in the medium. If the incident neutron has energy, U_0, then the kinetic energy in the medium is $U_0 - \langle V(\boldsymbol{x}) \rangle$. Therefore, the momenta can be calculated and we have

$$\text{Refractive index of neutron} = (1 - \langle V(\boldsymbol{x})\rangle / U_0)^{1/2}$$
$$= 1 - \frac{\rho_b \lambda^2}{2\pi} \tag{6.71}$$

where λ is the de Broglie wavelength, $h^2/(m_N v_0)^2$, in the vacuum (Exercise 6.25). The refractive index is less than unity for many medium ($\rho_b > 0$), so that vacuum is optically dense. The total external reflection is possible and neutrons can be guided by an evacuated tube, in which successive reflections occur.

Equations for light and x-ray scattering are equally applicable here. In particular, Eq. 6.63 can be rewritten for neutrons as follows:

$$I(q) = KN \cdot I_i |\rho_{b,p} - \rho_{b,s}|^2 \left| \int_V dV_j e^{i\boldsymbol{q}\cdot\boldsymbol{x}_j} \right|^2 \tag{6.72}$$

where I_i is the incident intensity and $\rho_{b,p}$ and $\rho_{b,s}$ are the scattering length densities of the particle and the solvent, respectively. Hence the scattering occurs when there is a difference in the scattering length density between the particle and the solvent. The same is also true for any part of the particle. We know that many interested molecules and particles have values of the scattering length density of the values between those of water and heavy water molecules. Thus, in a solution, if light and heavy water are properly mixed, a solvent can be produced to have the same scattering length density as that of the solute. Then, no scattering from the solute can be observed. The matching point of the scattering length densities can easily be obtained by plotting the square root of $I(q=0)$ against the mixing ratio of D_2O/H_2O, since this is a straight line from Eq. 6.72. If the solute has some structure, the detailed investigation of the structure may be possible by adjusting the contrast of the solvent. This is a powerful method, called the "contrast variation method". It was applied in micelles (Herbst et al., 1993). Nierlich et al. (1985) investigated the conformation of ionic polymers. A scattering peak from ionic pairs of polymers could be observed by van der Maarel et al. (1993). Sumaru et al. (1996) reported the ionic distribution around ionic spherical micelles. Yamaoka et al. (1995) replaced by deuterium either of the hydrophobic or hydrophilic part in micelles for investigation.

In a general case, the similar equation as Eq. 6.62 may have to be used for the analysis of the neutron scattring. For spherical particles of the identical size, we have

$$I(q) = KN \cdot I_i F(q) \left[1 + \frac{1}{N} \left\langle \sum_k \sum_{\neq k} e^{i\boldsymbol{q}\cdot(\boldsymbol{R}_k - \boldsymbol{R}_{k'})} \right] \right\rangle \tag{6.73}$$

For a dilute dispersion, this is reduced to Eq. 6.72.

Up to now we have always taken the spins of the incident neutrons to be randomly oriented, i.e. unpolarized. However, we can polarize the incident neutrons

and analyze the spin states of the scattered neutrons. Neutrons have magnetic moments, like tiny bar magnets. They can interact with electronic and nuclear magnetic moments. But nuclear magnetic moments are usually much smaller. Since the incident neutrons are moving, they see, in their own coordinate system, electrons and nuclei as moving charges in the targets. Moving charges always generate magnetic fields around. Electrons are orbiting around their own atomic nuclei. Thus, the incident neutrons magnetically interact with atoms and molecules. In addition, there is a relativistic effect, called the Foldy term (Lovesey, 1984), related to the zitterbewegung. Because of these interactions, the spin states of incident neutrons change at scattering. The spins can be precisely controlled under an external magnetic field and a technique called the neutron spin echo is a promising method for investigation of many problems in colloidal dispersions (Hayter, 1985).

6.5 Sedimentation Methods

Consider particles dispersed in a liquid. If the particle size is large ($>\sim 1$ μm), the liquid may be considered to be continuous. Then, a mechanical force, which acts on the mass, m_p, of a particle either under gravity or in a centrifuge, is given by $(m_p\text{-}m_l)\,g$ or $(m_p\text{-}m_l)\,\omega^2 x$, respectively, where m_l is the mass of the displaced liquid, g is the acceleration of gravity, ω is the angular velocity, and x is the radial distance of the particle from the center of the rotation. Clearly, if $m_p = m_l$ or the densities of the particle and the liquid are equal, the force vanishes. If it does not vanish, the particle will move with a speed v in the direction of gravity or radially against the viscous force γv (see Chapt. 4).

Gravity sedimentation is not feasible for particles below a few micrometers because of the violent Brownian motion. A centrifuge is then useful (between 60 nm and 3 μm), since the force can be easily increased by a factor of 10^5.

Under gravity, v almost instantly reaches a terminal speed v_t at infinite dilution when all the forces balance. We then have

$$v_t = (m_p - m_l)g/\gamma = 4\pi(\rho_p - \rho_l)a^3 g/(3\gamma) \tag{6.74}$$

where the particle is assumed to be a sphere of radius a and ρ's are densities. The coefficient, γ, is $6\pi a\eta$ under stick boundary conditions, where η is the viscosity of the liquid (see Eq. 4.21). Equation 6.74 holds for small Reynolds number ($\rho a v_t/\eta < 1$), when the inertia effects can be ignored. For $(\rho_p - \rho_l)/\rho_p \sim 1$ in water, it requires $a < 75$ μm. Note that v_t depends on the particle size, a.

The terminal speed, v_t, may be measured by using a laser Doppler velocimeter or anemometer to estimate m_p. Alternately, the speed may be measured under an ultramicroscope with timer.

At finite concentrations (φ: volume fraction) of identical hard spheres, the terminal speed is given by (Batchelor, 1972)

$$v = v_t[1 - 6.55\varphi + O(\varphi^2)] \tag{6.75}$$

due to partly the hydrodynamic backflow (–5.5φ), the pressure gradient (+0.5φ), and the near-field hydrodynamic effect (–1.55φ).

The experimental confirmation (Kops-Werkhoven et al., 1982) needs to show that the particles are hard spheres, by finding, for instant, that the second virial coefficient B of the osmotic pressure Π is 4 ($\Pi = nk_BT\{1+B\varphi+\cdots\}$, n: number density).

The sedimentation speed of Eq. 6.75 also depends on the nature of non-hydrodynamic interactions. For purely repulsive interactions of longer range than the radius of the hard sphere, the speed is reduced by increasing the retardation through backflow and reducing the near-field hydrodynamic interactions. Attraction, however, increases the sedimentation speed by the reversed reasons (Batchelor and Wen, 1982). Attraction also causes aggregation in sedimentation.

At finite concentrations ($\varphi \sim 0.5$ or less), experiments show the dependence given by (for instance, de Kruif et al., 1987))

$$v = v_t(1 - \varphi)^{-K}, \quad (K \sim -6.6 \text{ to } -5.4) \tag{6.76}$$

This result seems to hold for hard spheres. For strong attraction or repulsion, the volume fraction dependence could be much different.

As a dispersion settles in a closed container, the concentration gradient occurs, caused by compressibility imparted by the Brownian motion of and interactions among particles (Russel et al., 1989).

Spheres of unequal sizes settle with different velocities, complicating the sedimentation statistics. Any relative velocity induced by Stokes' settling velocities perturbs the balance between the interparticle interactions and Brownian motion (the diffusion coefficient D). The perturbation is characterized in terms of this velocity difference, Δv_t, by defining a Peclet number for sedimentation,

$$Pe = 2a\Delta v_t/D = [8\pi a^4(\rho_p - \rho_l)g/3k_BT](\Delta v_t/v_t) \tag{6.77}$$

(a=averaged radius). For $Pe \ll 1$, the perbation is small. For $Pe \gg 1$, the hydrodynamic forces dominate Brownian motion and determine the microstructure of sedimentation in polydisperse suspension. Hence the concentration dependence of the sedimentation velocity for macroscopic particles can differ substantially from that for small particles. Batchelor and Wen (1982) studied the perturbation and the experimental results of Davis and Birdsell (1988) showed a good agreement.

If particles in a liquid is smaller than 1 μm, the Brownian motion may interfere with the sedimentation (Sec. 12.5). In particular, when a small particle moves in a gas (aerosols), Brownian motion is noticeable and the value of γ needs to be cor-

rected for Eq. 6.74 to be used. This effect was, historically observed in the famous Millikan experiment on the electronic charge.

In a centrifuge, when the forces balance,

$$(m_p - m_l)\omega^2 x = \gamma \mathrm{d}x/\mathrm{d}t$$

The time spent by the particle in travelling radially from x_0 to x is given by

$$t - t_0 = \gamma \ln(x/x_0)/[(m_p - m_l)\omega^2] \tag{6.78}$$

Experimentally, a suspension is injected at x_0 into a centrifuge while it is spinning with the liquid. Assuming that the dispersed particles instantly attain the terminal speed, the time, t–t_0, is measured by optically detecting them at $x > x_0$. Thus the rotor is usually made transparent.

From either Eq. 6.74 or 6.78, the size of the particle m_p or a can be found, provided the effect of diffusion is small.

6.6 The Coulter Counter

This is an electrical pulse counter, which was originally designed simply to count the number of particles in a known volume of an electrolyte solution ($\sim$5 per cent salt) by drawing the suspension through a small orifice that had an electrode on the either side of it. If a particle flows between the electrodes, the electric resistance changes and the current can be amplified as a voltage pulse and counted.

This counter is very useful for the determination of the particle volume size and its distribution at the larger end of the particle size range (>0.6 μm), provided the particles are less electrically conductive and are able to stand the shearing forces while being drawn through an orifice. The counter has been used to measure floc sizes (Hunter and Frayne, 1980).

We assume that the instrument is calibrated with dispersions of a known particle-volume size v_c, such that the pulse height, t_c, is proportional to v_c.

$$v_c = k_1 t_c \tag{6.79}$$

This can be easily experimentally checked, provided one avoids the complication of coincidence and works within the recommended size rage (from a diameter of about 40 per cent of the orifice diameter down to 2 percent). The volume of an unknown particle can then be determined from the pulse height.

The minimum size of the orifice in a workable instrument is about 16 μm diameter (the minimum measurable size is about 0.3 μm). However, 30 μm may be more appropriate to avoid coincidence. The counter works up to the orifice diame-

ter of 1000 μm (maximum measurable size: 400 μm). The concentration of sol must also be kept low, otherwise a correction is required against coincidence.

The theory of Eq. 6.79 is as follows. If the cross-sectional area of the orifice opened on a partition of thickness of δl is A and the resistivity of the fluid is ρ, the resistance between two electrodes across the orifice is given by

$$R_0 = \rho \cdot \delta l / A$$

If the particle has the cross-sectional area, A_p, and if it is faraway from the orifice wall, this resistance increases to $R = \rho \cdot \delta l / (A - A_p)$, so that the change is given by

$$\delta R = \rho \cdot \delta l \left(\frac{1}{A - A_p} - \frac{1}{A} \right) = \frac{\rho \cdot A_p \cdot \delta l}{A^2} \left(1 - \frac{A_p}{A} \right)^{-1} \tag{6.80}$$

The pulse height is, therefore, not strictly proportional to particle volume ($A_p \cdot \delta l$).

The pulse shape has some effect on the counts. If the particle moves near the orifice wall, double peaks may result due to hydrodynamic effect. Such a case must be rejected from the result of counting.

6.7 Hydrodynamic Chromatography (HDC)

Another method of the particle sizing is the use of hydrodynamic chromatography, which works well for a stable solution. When a solution is injected into a stream of liquid flowing through a column packed with small solid spheres ($\sim$10 μm), the particles separate according to the size, with the largest particles eluting first. The size is calibrated with a colloidal solute of known molecular weight, or measured optically. Thus, some colloids are characterized by molecular weight, which can be easily converted to their geometrical sizes if the density is known. Chromatography provides a rapid method for fractionating polydisperse systems and is capable of size separation of particles between 20 nm and 1 μm.

The subsequent size analysis is made more reliable than that of the original unseparated sample.

The dispersed solution may be forced under pressure ($\sim$20 atm.) through the packed column.

Large particles travel through the column more rapidly than small ones. Stoisits et al. (1976) measured the ratio R:

$$R = \frac{\text{Rate of transport of colloid through column}}{\text{Rate of transport of elution fluid}} \tag{6.81}$$

and found that R varied roughly from 1.02 and 1.11. They assumed a mechanical model that the column was approximated by a combination of many small paral-

lel cylindrical pores. The flow speed profile in the pore is given by the Poiseuille equation:

$$v(r) = \frac{\Delta P r_0^2}{4\eta l}\left[1 - \left(\frac{r}{r_0}\right)^2\right] \tag{6.82}$$

where r is measured radially from the center of the cylindrical pore of radius r_0, ΔP is the pressure drop along the cylinder of length l. The maximum speed v_0 occurs along the axis and zero at the wall. The average speed is equal to $v_0/2$. The center of a sphere of radius a is located at a distance b from the axis ($0 < b < r_0 - a$). The force and the torque acting on this sphere has been calculated (Happel and Brenner, 1973) and the speed of the particle is $v_p = v(b)$. The average is given by

$$\langle v_p \rangle = v_0[1 - (1/2)(1 - (a/r_0))^2] \tag{6.83}$$

Therefore, we find that

$$R = \langle v_p \rangle / \langle v(r) \rangle = 2 - (a/r_0)^2 \tag{6.84}$$

where $\langle v(r) \rangle$ is the average of the Poiseuille flow speed, $v_0/2$. Equation 6.83 shows that, if a ($< r_0$) is larger, the elusion is faster.

Exercises

6.1 Why do not we have an x-ray microscope? (Hint: refractive index sensitive to medium.)

6.2 What is the de Broglie wavelength of an electron which is accelerated by 200 kV? Should it be treated relativistically? Note that the wavelength, λ, is given by h/p, where h is Planck's constant and p is the electron momentum, or

$$\lambda = \frac{h}{(2mE)^{1/2}\left(1 + \frac{E}{2mc^2}\right)}$$

where m and E are the mass and the kinetic energy of the electron, respectively, and c is the speed of light.

6.3 Consider a polarizable spherical particle. The induced dipole moment has the same direction as the polarization vector of an incident linearly polarized light. From the simple vectorial relation, find the intensity relation of the scattered light of the vertical incident light and that of the horizontal incident light (see Eq. 6.1).

6.4 Suppose that we like to apply, as a good approximation, the Rayleigh scattering formula to a small nonspherical particle, such as an ellipsoid, which does not carry any

permanent electric dipole moment. What expression should be used to replace Eq. 4.91? (Calculate the polarizability tensor and average over the orientation.)

6.5 The particle polarizability, α, appearing in Eq. 4.91 is for the vacuum environment. Obtain the polarizability so that it can be applicable when the particle is in a medium of dielectric constant, ε_m, and exposed to $\boldsymbol{E}$ (Eq. 4.88) in a medium of dielectric constant, ε_m. (This polarizability is called the excess polarizability since the particle is replacing the medium by the same volume. See Landau and Lifshitz, 1963.) But, in scattering, we must refer to the external field, $\boldsymbol{E}$, so that the particle exposed to $\boldsymbol{E}/\varepsilon_m$ in a dielectric, when the external field is $\boldsymbol{E}$, if the solution is dilute. Then, noting that the dielectric constant, ε_s, of the solution (with the particles as a solute) is equal to the refractive index, n_s^2, and, similarly, $\varepsilon_m = n_m^2$ for the medium (solvent), express the effective α in terms of the refractive indices of the solution and solvent.

6.6 Consider N_p particles per unit volume in the surrounding medium of refractive index n_m. That of the solution is n_s. The particles have a particle polarizability of α (see Exercise 6.5). Following Eqs. 4.88 and 4.90, show that

$$\boldsymbol{\alpha} = 3\varepsilon_0 \frac{n_s^2 - n_m^2}{(n_s^2 + 2n_m^2)N_p}$$

Then, also show that, if $n_s \sim n_m$, $\alpha = 2\varepsilon_0 (n_s - n_m)/(n_m N_p)$ for a dilute solution.

6.7 What will be observed in scattering when Brownian particles in a liquid are irradiated by light of a very narrow frequency which is the atomic resonance frequency of the particles at rest? (The liftime of the atomic radiation process is of the order of 10^{-8} s but the mean free time of the particles is much shorter. What happens if particles are fast moving without collision in free space under the irradiation of the light?)

6.8 Establish the conditions under which Eq. 6.11 holds, provided Eq. 6.9 is correct. Note that

$$e^{i\boldsymbol{k}\cdot\boldsymbol{r}} = \sum_{l=0}^{\infty} (2l+1) i^l j_l(kr) P_l(\cos\theta)$$

where $i = (-1)^{1/2}$ and $j_l(kr)$ and $P_l(\cos\theta)$ are, respectively, the spherical Bessel function and the Legendre polynomial of the l-th order, respectively. The symbol, θ, is the angle between $\boldsymbol{k}$ and $\boldsymbol{r}$, and $j_o = \sin(kr)/(kr)$, etc.

6.9 Show that the Debye factor $P(\theta) \to 1$ as $\theta \to 0$.

6.10 Suppose that an infinitely long wave train of amplitude, A, and frequency, ω_0, is abruptly chopped to a finite length of T in time. Then, the frequency components involved in this chopped wave are given by

$$f(\omega) = \frac{1}{(2\pi)^{1/2} T} \int_0^T e^{i\omega_0 t} e^{-i\omega t} d\omega$$

Briefly plot the frequency distribution.

6.11 If the incident beam of a circular cylinder has a width of 0.1 cm, what will be A_{coh} at $R = 1$ m? (The beam size determines that of the scattering volume. Use Eq. 6.16.)

6.12 Find the transformation laws of a vector and a tensor of rank 2. (Transformations from one to another Cartesian coordinates with direction cosines, α, β, γ.)

6.13 Consider light scattering from gas molecules at a temperature T. Find the line width due to the Doppler broadening. (The Doppler frequency shift is goven by $\boldsymbol{q}\cdot\boldsymbol{v}$ from Eq. 6.13. The particle velocity $\boldsymbol{v}$ distributes according to the Maxwell distribution function.)

6.14 In analysis of the scattered wave from Brownian particles, why useful is the optical method, if the intensity variation is too fast for the electronic method by means of a photomultiplier? (The optical method changes the temporal variation to a wavelength (or frequency) variation, which is optically detectable. The lifetime of a very rapid γ emission can be very often measured optically.)

6.15 If $\boldsymbol{E}(t)=\Sigma_j \mathbf{E}_j \exp\{i(\omega_0 t+\phi_j(t)\}$ at the photocathode of a photomultiplier, where $\phi_j(t)$ is a random phase shift, show that the output current fluctuates in time. (The number n of photoelectrons during a short sampling time is proportional to the light intensity at the photocathode and to the output current. Follow the outline of Eq. 6.14.)

6.16 Consider an oscillating electric dipole moment $p(t)=e\cdot x(t)$, where e is the point charge and $x(t)$ is its displacement.

$$p(t) = p_0 \exp\left[-i\int_0^t \omega(t')\mathrm{d}t'\right]$$

The power radiated is $(1/6\pi\varepsilon_0)e^2c^{-3}(\mathrm{d}^2x/\mathrm{d}t^2)^2$. Establish Eq. 6.19.

6.17 Show that the diagonal sum or trace of the polarizability tensor is invariant under rotation.

6.18 Establish Eqs. 6.27 and 6.28.

6.19 Establish the correlation functions, Eqs. 6.29 and 6.30.

6.20 Obtain Eqs. 6.46 and 6.51.

6.21 The target used in an x-ray tube is usually metallic. Why is the target metallic? (X-rays are emitted by bombarding electrons.)

6.22 Since the synchrotron radiation of various wavelengths is available, an x-ray of longer wavelengths may be used to investigate the size and structure of small particles at a comfortably larger scattering angle. Why is this not so popular? (Consider in terms of absorption of soft x-rays in matter.)

6.23 Show that $\boldsymbol{x}_j$ of Eq. 6.54 must refer to the coordinates with the origin at the center of symmetry.

6.24 Calculate the neutron scattering length density for D_2O.

6.25 Establish Eq. 6.71. Find the refractive index of water for thermal neutrons.

6.26 Why is the electron scattering not used for sizing in disperse suspensions?

6.27 Derive Eqs. 6.83 and 6.84.

References

Ancellet, G.M. and Menzies, R.T., *J. Opt. Soc. Amm. A*, *4*, 367 (1987).
Ashdown, S., Markovié, I., and Ottewill, R.H., *Langmuir 6*, 303 (1990).
Bale, H.D. and Schmidt, P.W., *Phys. Rev. Lett. 53*, 596 (1984).

Batchelor, G.K., *J. Fluid Mech. 52*, 245 (1972).
Batchelor, G.K. and Wen, C.S., *J. Fluid Mech. 124*, 495 (1982).
Berne, B.C. and Pecora, R., "Dynamic Light Scattering", John Wiley & Sons, Inc., New York (1976).
Binning, G., Quate. C.F., and Gerber, C., *Phys. Rev. Lett. 56*, 930 (1986).
Binning, G., Rohrer, H., Gerber, C., and Weibel, E., *Phys. Rev. Lett. 49*, 50 (1982).
Chen, S.H., Holz, M., and Tartaglia, P., *Appl. Opt. 16*, 187 (1977).
Ch'en, S.Y. and Takeo, M., *Rev. Mod. Phys. 29*, 20 (1957).
Chu, B., "Laser Light Scattering", 2nd ed., Academic Press, Inc., San Diego (1991).
Cummins, P.G., Staples, E.J., Thompson, L.G., and Pope, L., *J. Colloid Interface Sci. 92*, 189 (1983).
de Kruif, C.G., Jansen, J.W., and Vrij, A., in "Physics of Complex and Supramolecular Fluids", eds. S.A. Safron, and N.A. Clark, Wiley-Interscience, New York (1987), p. 315.
Debye, P., *J. Phys. and Colloid Chem. 51*, 81 (1947).
Davis, R.H. and Birdsell, K.H., *AIChE J. 34*, 123 (1988).
Edmunds, A.R., "Angular Momentum in Quantum Mechanics", Princeton University Press, Princeton (1957).
Evans, J.M., in Huglin, M.B., ed., "Light Scattering From Polymer Solutions", Academic Press, London and New York (1972).
Fontana, M. Rustichelli, and Coppola, R., eds., "Industrial and Technological Applications of Neutrons", North-Holland, Amsterdam (1992).
Fournet, G., *Bull. Soc. Fr. Mineral. Cristallogr. 74*, 39 (1951).
Friman, R. and Rosenholm, J.B., *Colloid. Polym. Sci. 260*, 545 (1982).
Garcia-Rubio, L.H., in "Particle Size Distribution", ed., Provder, T., American Chemical Society, Washington, DC (1987), p. 162.
Guinier, A., *Ann. Phys. 12*, 161 (1939).
Happel, J. and Brenner, H., "Low Reynolds number hydrodynamics", Noordhoff International Publishing, Leiden, Netherlands (1973), p. 314.
Hashimoto, T., Fujimura, M., and Kawai, H., *Macromolecules 13*, 1660 (1980).
Hayter, J.B., in "Physics of amphiphiles: micelles, vesicles and microemulsions", eds., Degiorgio, V. and Corti, M., North-Holland, Amsterdam (1985).
Henon, S. and Meunier, J., *Rev. Sci. Instr. 62*, 936 (1991).
Herbst, L., Kalus, J., and Schmelzer, U., *J. Phys. Chem. 97*, 7774 (1993).
Hiemenz, P.C., "Principles of Colloid and Surface Chemistry", 2nd ed., Marcel Decker, New York (1986).
Hönig, D. and Möbius, D., *J. Phys. Chem. 95*, 4590 (1991).
Hunter, R.J. and Frayne, J., *J. Colloid Interface Sci. 76*, 107 (1980).
J. Physique IV, Colloque, C8 (1993). This is Proceedings of the international conference on applications of small-angle scattering.
Jackson, J.D., "Classical Electrodynamics", 2nd ed., John Wiley & Sons, Inc., New York (1975).
Jakeman, E., Oliver, C.J., and Pike, E.R., *J. Phys. A 3*, L45 (1970).
Jiang, S., Tomita, N., Ohsawa, H., and Ohtsu, M., *Jpn J. Appl. Phys. 30*, 2107 (1991).
Kerker, M., "The scattering of light and other electromagnetic radiation", Academic Press, New York (1969).
Kops-Werkhoven, M.M., Pathmamanoharan, C., Vrij, A., and Fijnaut, H.M, *J. Chem. Phys. 77*, 5913 (1982).
Kratky, O. and Glatter, O., "Small-angle X-ray Scattering", Academic Press, New York (1982).
Kratky, O. and Porod, G., *J. Colloid Sci. 4*, 35 (1949).
Landau, L.D. and Lifshitz, E.M., "Electrodynamics of Continuos Media", vol. 8, 2nd ed., Pergamon, Oxford (1963).
Lovesey, S.W., "Theory of Neutron Scattering from Condensed Matter", Vols. 1 and 2, Clarendon Press, Oxford (1984).
Marignan, J., Basserau, P. and Delord, P., *J. Phys. Chem. 90*, 645 (1986).
Martin, Y. and Wickramasinghe, H.K., *Appl. Phys. Lett. 50*, 1455 (1987).
Martin,Y., Abraham, D.W., and Wickramasinghe, H.K., *Appl. Phys. Lett. 52*, 1103 (1988).
Mate, C.M., McClelland, G.M., Erlandsson, R., and Chiang, S., *Phys. Rev. Lett. 59*, 1942 (1987).

Matsuoka, H., Schwahn, D., and Ise, N., in "Macro-ion Characterization, from Dilute Solutions to Complex Fluids", ed. Schmitz, K.S., ACS Symposium Series 548, American Chemical Society, Washington D.C. (1994).
Matsuoka, H., Tsurumi, M., and Ise, N., *Phys. Rev. B. 38*, 6279 (1988).
Mie, G., *Ann. Phys. (Leipzig) 25*, 377 (1908).
Muramatsu, H., Chiba, N., Homma, K., Nakajima, K., Ataka, T., Ohta, S., Kusumi, A., and Fujihira, M., *Appl. Phys. Lett. 66*, 3245 (1995).
Nakanishi, K., Soga, N., Matsuoka, H., and Ise, N., *J. Am. Ceram. Soc. 75*, 971 (1992).
Neugebauer, T., *Ann. Physik 42*, 509 (1943).
Nierlich, M. et al., *J. Physique 46*, 649 (1985).
Pecora, R., Ed., "Dynamic Light Scattering", Plenum Press, New York and London (1985).
Pohl, D.W. and Courjon, D., eds., "Near Field Optics", Kluwer Academic Publisher, Dordrecht (1993).
Porod, G., *Kolloid-Z. 124*, 83 (1951).
Pusey, P.N., in "Colloidal dispersion", ed., Goodwin, J.W., Royal Society of Chemistry, London (1982).
Rayleigh, Lord, *Proc. Roy. Soc. A90*, 219 (1914).
Russel, W.B., Saville, D.A., and Schowalter, W.R., "Colloidal Dispersions", Cambridge University Press, Cambridge (1989).
Saenz, J.J., Garcia, N., Grütter, P., Meyer, E., Heinzelmann, H., Wiesendanger, R., Rosebthaler, L., Hidber, H.R., and Güntherodt, H.-J., *J. Appl. Phys. 62*, 4293 (1987).
Schaefer, D.W., *Science 243*, 1023 (1989).
Schmidt, P.W., "The Fractal Approach to Heterogeneous Chemistry – Surfaces, Colloids, Polymers", ed., Avnir, D., Chapt. 2, John Wiley & Sons (1989).
Schnablegger ,H. and Glatter, O., *Applied Optics 30*, 4889 (1991).
Sears, V.F., *Neutron News 3*, 26 (1992).
Silverman, L., Billings, C.E., and First, M.W., "Particle size analysis in industrial hygiene", Academic Press, New York (1971).
Stoisits, R.F., Pehlein, G.W., and Vanderhoff, J.W., *J. Colloid Interface Sci. 57*, 337 (1976).
Sumaru, K., Matsuoka, H., Yamaoka, H., and Wignal, G.D., *Phys. Rev. E 53*, 1744 (1996).
Synge, E.H., *Phil. Mag. 6*, 356 (1928).
van der Maarel, J.R., Groot, L.C.A., Hollander, J.G., Sesse, W., Kuill, M.E., Leyte-Zuiderweg, L.H., and Mandel, M., *Macromolecules 26*, 7295 1993.
Vrij, A., Nieuwenhuis, E.A., Fijnaut, H.M., and Agterof, W.G.M., in "Colloid Stability", *Faraday Disc. Chem. Soc. 65*, The Chemical Society, London (1978).
Watson, R.M.J. and Jennings, B.R., *J. Colloid Interface Sci. 142*, 244 (1991).
Watson, R.M.J. and Jennings, B.R., *J. Colloid Interface Sci. 157*, 361 (1993).
Weiner, B.B., in "Modern Methods in Particle Size Analysis", ed., Barth, H.G., Wiley, New York (1984).
Yamaoka, H., Matsuoka, H., Sumaru, K., Hanada, S., Imai, M., and Wignal, G.D., *Physica B 213/214*, 700 (1995).
Zemb, T. and Charpin, P., *J. Physique 46*, 249 (1985).
Zimm, B.H., *J. Chem. Phys. 16*, 1093 (1948).